

## Gravity Model Development for TOPEX/POSEIDON: Joint Gravity Models 1 and 2

R. S. Nerem,<sup>1</sup> F. J. Lerch,<sup>1</sup> J. A. Marshall,<sup>1</sup> E. C. Pavlis,<sup>2</sup> B. H. Putney,<sup>1</sup> B. D. Tapley,<sup>3</sup>  
R. J. Eanes,<sup>3</sup> J. C. Ries,<sup>3</sup> B. E. Schutz,<sup>3</sup> C. K. Shum,<sup>3</sup> M. M. Watkins,<sup>3</sup> S. M. Klosko,<sup>4</sup> J. C.  
Chan,<sup>4</sup> S. B. Luthcke,<sup>4</sup> G. B. Patel,<sup>4</sup> N. K. Pavlis,<sup>4</sup> R. G. Williamson,<sup>4</sup> R. H. Rapp,<sup>5</sup>  
R. Biancale,<sup>6</sup> and F. Nouel<sup>6</sup>

**Abstract.** The TOPEX/POSEIDON (T/P) prelaunch Joint Gravity Model-1 (JGM-1) and the postlaunch JGM-2 Earth gravitational models have been developed to support precision orbit determination for T/P. Each of these models is complete to degree 70 in spherical harmonics and was computed from a combination of satellite tracking data, satellite altimetry, and surface gravimetry. While improved orbit determination accuracies for T/P have driven the improvements in the models, the models are general in application and also provide an improved geoid for oceanographic computations. The postlaunch model, JGM-2, which includes T/P satellite laser ranging (SLR) and Doppler orbitography and radiopositioning integrated by satellite (DORIS) tracking data, introduces radial orbit errors for T/P that are only 2 cm RMS with the commission errors of the marine geoid for terms to degree 70 being  $\pm 25$  cm. Errors in modeling the nonconservative forces acting on T/P increase the total radial errors to only 3-4 cm RMS, a result much better than premission goals. While the orbit accuracy goal for T/P has been far surpassed, geoid errors still prevent the absolute determination of the ocean dynamic topography for wavelengths shorter than about 2500 km. Only a dedicated gravitational field satellite mission will likely provide the necessary improvement in the geoid.

### Introduction

The exploitation of satellite altimetry requires the precise knowledge of the Earth's gravitational field for two reasons: (1) accurate determination of the satellite position is required to measure the height of the sea surface using altimeter range measurements, and (2) the geoid, an equipotential surface of the gravity field corresponding to mean sea level, is required as a reference surface for the computation of the ocean dynamic topography whose slope is directly related to the geostrophic velocity of the ocean currents [Wunsch and Gaposchkin, 1980]. When the TOPEX/POSEIDON (T/P) mission was first conceived in the early 1980s [TOPEX Science Working Group, 1981], the best long-wavelength Earth gravitational models available at that time, Goddard Earth Model (GEM) GEM-10B [Lerch *et al.*, 1979] and GEM-L2 [Lerch *et al.*, 1982], were

predicted to cause RMS radial orbit errors for T/P of more than 50 cm. Gravity was known to be the dominant error source for determining the T/P orbit. Recognizing that, a multi-institutional research team began developing improved Earth gravitational models with a goal of reducing the radial orbit errors from the geopotential for T/P to 10 cm RMS or less as specified in the mission error budget [Stewart *et al.*, 1986].

Over the last decade, a series of Earth gravitational models have been developed out of this focused research effort; each field progressively moved closer to the T/P 10 cm goal. These models include GEM-T1 [Marsh *et al.*, 1988], TEG-2 [Shum *et al.*, 1990], GEM-T2 [Marsh *et al.*, 1990a], TEG-2B [Tapley *et al.*, 1991], GEM-T3 [Lerch *et al.*, 1994]; and GEM-T3A [Nerem *et al.*, 1994a]. A summary of this progress is given by Lerch *et al.* [1993b]. Additional models which have been developed outside of the T/P effort are GRIM4-C3 [Schwintzer *et al.*, 1991], OSU89A/B [Rapp and Pavlis, 1990], and OSU91A [Rapp *et al.*, 1991]. Herein we describe the final results of this research effort, the prelaunch field Joint Gravity Model-1 (JGM-1, also in honor of our late colleague James G. Marsh), and the postlaunch field JGM-2, which differs from JGM-1 principally through the addition of T/P tracking data.

Orbit determination can be simply stated as the adjustment of the orbit state, force, and measurement model parameters to minimize, in a least squares sense, the weighted difference between the actual tracking observations and their predicted values. Clearly, the accuracy of the computed orbit will depend on the accuracy and completeness of the force models, the measurement models, and the tracking data. In principle, T/P contains five tracking systems which can be used for determining its orbit [Nerem *et al.*, 1993a]: (1) satellite laser ranging (SLR) [Degnan, 1993]; (2) Doppler orbitography and radiopo-

<sup>1</sup> Space Geodesy Branch, NASA Goddard Space Flight Center, Greenbelt, MD.

<sup>2</sup> Department of Astronomy, University of Maryland, College Park, MD.

<sup>3</sup> Center for Space Research, University of Texas at Austin, Austin, TX.

<sup>4</sup> Hughes STX Corporation, Lanham, MD.

<sup>5</sup> Department of Geodetic Science and Surveying, Ohio State University, Columbus, OH.

<sup>6</sup> Centre Nationale d'Etudes Spatiales, Toulouse, France.

Copyright 1994 by the American Geophysical Union.

Paper number 94JC01376.

0148-0227/94/94JC-01376\$05.00

sitioning integrated by satellite (DORIS) tracking data [Nouel *et al.*, 1988; Cazenave *et al.*, 1992]; (3) Global Positioning System (GPS) tracking data [Bertiger *et al.*, this issue; Melbourne *et al.*, 1994; Yunck *et al.*, 1994; Schutz *et al.*, 1994]; (4) the Tracking and Data Relay Satellite System (TDRSS) [Schanzle *et al.*, 1992]; and (5) the satellite altimeter measurements themselves [e.g., Tapley *et al.*, 1988; Nerem *et al.*, 1990; Marsh *et al.*, 1990b]. For the orbits which the National Aeronautics and Space Administration/Goddard Space Flight Center (NASA/GSFC) computes for the T/P altimeter geophysical data records (GDRs), only the well-tested and ocean-surface-independent SLR and DORIS data types are being used initially. The SLR and DORIS data are complementary; the SLR data provide precise slant-range information from a global set of tracking stations which are somewhat limited in geographic extent; the DORIS data provide precise line-of-sight velocity information from an extensive global network of stations which track the satellite nearly continuously. Both of these data types have in the past been very important for determining the gravity field; the use of these data types for T/P directly in the gravity solution provides extensive sensing of gravitational effects specific to the T/P orbit, such as long-term zonal, monthly, and resonant perturbations [Kaula, 1966].

As indicated in the orbit determination error budget [Stewart *et al.*, 1986; Tapley *et al.*, this issue], precise modeling of the Earth's gravitational field was only one of many activities necessary to meet the stringent requirements for T/P. The precise modeling of nonconservative forces due to solar/Earth radiation pressure, thermal imbalances, atmospheric drag, and spacecraft emissions required intensive parallel study [Marshall and Luthcke, 1994; Nerem *et al.*, 1993a] and resulted in the development of a complex box-wing model describing the forces acting on each plate of a rectangular spacecraft model (the box) and the solar array (the wing). A subset of parameters describing the box-wing model were solved for simultaneously with the gravity field coefficients in the JGM-2 solution. The high-quality precision orbit determination results using SLR/DORIS tracking data, the box-wing nonconservative force model, and the JGM-2 gravity model are extensively discussed by Tapley *et al.* [this issue].

### JGM Model Development

The most comprehensive of the "T/P-era" gravity models have been formed from a combination of satellite tracking data, surface gravimetry and satellite altimetry observations [Lerch *et al.*, 1994; Tapley *et al.*, 1991; Rapp *et al.*, 1991; Schwintzer *et al.*, 1991]. These models were constructed from data having widely varying accuracy and spectral sensitivity to the gravitational signal. Rigorous statistical techniques have been developed to optimally combine these data and produce realistic accuracy estimates. The T/P-era modeling efforts have been in the forefront of developing calibration and optimal data weighting techniques to enable systematic errors in specific data sets to be better understood [Lerch *et al.*, 1985; Lerch, 1991; Lerch *et al.*, 1991; Lerch *et al.*, 1993a; Yuan, 1991].

With the completion of the GEM-T3-class of models [Lerch *et al.*, 1994; Nerem *et al.*, 1994a], it was decided to reiterate the gravity model solution by reprocessing all of the data using GEM-T3 as the a priori gravity model and an improved set of background models and constants. The reiteration is a sizable computational effort but is necessary due to the nonlinearities in the gravity field estimation problem and implementation of

improvements in adopted parameters. The first few steps include preprocessing, data quality control, and data compression into normal points. Data arcs are selected up to 1 month in length (e.g., LAGEOS, Etalon-1), but shorter arcs are used for lower satellites. These data are reduced using a complex set of a priori models through a weighted least squares adjustment of the parameters defining the spacecraft state, the force model, and the measurement model. When an arc of data is satisfactorily reduced, edited, and the data qualified, a system of normal equations is generated for all orbital and geodetic parameters of interest. The solution is based on the combination of all of these normal equations using an optimal weighting scheme. A set of parameters are selected for estimation, the reduced matrix is inverted, and the solution with its accompanying statistics are then evaluated.

The strategy of developing "satellite-only" (models based only on satellite tracking data) and "combination" solutions (models based on satellite tracking data, altimeter data, and surface gravity data) was continued with the JGM models. This approach provides better insight into subtle data incompatibilities existing between tracking, surface gravimetry and altimeter observations. These incompatibilities significantly affect the weight given to altimeter and surface gravity data sets in the solution, and the resulting down-weighting of these data prevent their full exploitation within comprehensive solutions. Significant efforts have transpired to improve our modeling of these data to enable them to be more fully exploited within the JGM solutions. Improvements in ancillary models and data treatment were also implemented to better isolate the gravitational signal.

The series of gravitational models developed in anticipation of the T/P mission and the computational techniques employed are well documented in the open literature. Details of these procedures are given by Marsh *et al.* [1988, 1990a, 1990b]; Lerch *et al.* [1991, 1993a, 1993b, 1994]; Nerem *et al.* [1990, 1994a]; Tapley *et al.* [1988]; Shum *et al.* [1990]; and Yuan [1991]. However, the development of the JGM models necessitated significant changes in some approaches and these are briefly reviewed below.

The JGM models are complete to degree and order 70 in spherical harmonics, corresponding to a half-wavelength spatial resolution of approximately 300 km. A field of this size (benefiting from the attenuation of the gravity signal at altitude) completely accommodates all satellite orbital perturbations sensed by the tracking data used in the solution. All of the altimeter data and surface gravimetry were corrected for the contribution of the high degree and order gravity field from degrees 71 to 360. This approach reduced the aliasing arising from field truncation within the solution from these data sets which contain strong short wavelength geopotential signal. The OSU91A geopotential model [Rapp *et al.*, 1991], a field complete to degree 360, was utilized to perform these corrections.

Previous T/P-era models have unrealistically low power in the high degree portion of the field due to the use of a priori coefficient constraints. The necessity for this conditioning was eliminated in the JGM series of solutions by using isotatic/topographic prediction methods to fill in all unobserved mean gravity anomaly blocks [Rapp and Pavlis, 1990]. With a complete grid of surface anomalies, the short wavelengths in the geopotential were globally defined, thus eliminating the need to constrain local field adjustments over previously unobserved regions.

Although the available surface gravity data are of nonuniform quality and coverage and lack long-wavelength integrity due to a number of systematic errors [Heck, 1990], these data are unique for defining the intermediate and short-wavelength field over the continents. A second innovation in the JGM solutions provided for a separate degree and order 5 long-wavelength geopotential model to be simultaneously estimated exclusively from the surface gravimetry. This approach permitted these data to receive greater weight in the JGM solutions and reduced the aliasing in the overall model due to long wavelength error caused by datum and vertical reference system problems commonly seen within surface gravimetric data [cf. Rapp, 1983].

### Background Models

The constants and reference frame which were adopted and used in the development of the JGM models delineate the physical frame within which the solution was computed. Given the specific needs of T/P, the consistency and time dependence of these parameters over the projected 5-year lifetime of the mission were of considerable interest. The reiteration saw the introduction of a refined set of constants and ancillary models and was designed to take advantage of the extensive experience acquired in producing the previous models. Because this gravity field solution required the reduction of a large and diverse database encompassing over 30 satellites and millions of observations acquired over a 30-year period, the time dependent nature of the reference frame and constants permeated the JGM modeling efforts. Data analysis and ancillary force modeling improvements were instituted to better isolate the gravitational signal from other sources of orbit perturbations. Improved models for the ocean tides, relativity, and the time dependent motion of stations within our Conventional Terrestrial Reference System were also introduced.

Temporal variations of the external gravitational field arise from a number of different geophysical phenomena [Chao, 1993]. They occur at a variety of spatial and temporal scales, ranging from episodic variations due to earthquakes to secular variations related to postglacial rebound or mean sea level rise. Since the data contained in the JGM models span nearly three decades, consideration of temporal variations in gravity are a necessary part of the development of the solutions.

Nontidal temporal variations of the gravitational field represent a dynamic aspect of the mass redistribution within the solid-Earth/ocean/atmosphere system. Nontidal gravitational perturbations are manifestations of complex geophysical processes and interactions within these systems; mass redistribution of this character is generally not sufficiently well known to be applied as a priori information in the development of the JGM models. However, a LAGEOS-based value of the secular change in  $J_2$  (where  $J_2 = -\sqrt{5} C_{2,0}$ ) of  $-2.6 \times 10^{-11}/\text{yr}$  [Nerem et al., 1993b], which is similar to results previously reported by Rubincam [1984], Cheng et al. [1989] and Yoder et al. [1983], was adopted for the JGM models. This value was determined with respect to an equilibrium value for the 18.6-year lunar tide which was also adopted for the first time within the JGM solutions.

A distinct category of temporal gravity variations is of tidal origin and occurs at well-defined astronomical frequencies and is currently well modeled at the long-wavelengths where satellites are sensitive [cf. Christodoulidis et al., 1988]. The tides were extensively studied and expanded models were produced

and used for a priori modeling to properly account for these effects over the interval encompassed by the tracking data and for future orbit recovery applications. Highlights of the improvements instituted are as follows.

Both tidal and nontidal sources of mass redistribution required considerable attention in the JGM solutions, for these effects may not effectively average to zero when recovering the static field, and their modeling is required within precise orbit computations. The consistency of the T/P orbit accuracy from arc to arc and limiting distortions arising from unmodeled long-period effects in the reference frame over a 3- to 5-year T/P mission lifetime was an important consideration; the accurate monitoring of interannual ocean processes with respect to a consistent reference orbit using the T/P altimeter data is a major objective.

### Ocean Tide Modeling

Tide modeling within orbit determination and gravity solutions entails the following:

1. Improving the long-wavelength tidal terms which are in orbital resonance giving rise to sizable long-period orbit perturbations. Recent geopotential solutions have directly estimated a set of resonant spherical harmonic terms in the tidal expansion for major tidal constituents [cf. Marsh et al., 1988; 1990a; Christodoulidis et al., 1988; Cheng et al., 1992].

2. Incorporating a large number of harmonic coefficients spanning many tide lines which give rise to short-period orbital perturbations. The task here is to select those terms which need to be included in order to reduce omission errors to some satisfactory level. On the basis of an orbital sensitivity analysis [cf. Casotto, 1989], these omission errors were kept below the 1-cm level in their root-sum-square (rss) radial contribution to the T/P orbit [Nerem et al., 1993a].

Generally, the coefficients defining the gravity model and the ocean tides are adjusted simultaneously. Unfortunately, due to a computer programming error in defining sideband tidal contributions, the JGM normal equations for the ocean tides could not be satisfactorily adjusted and thus their values were held fixed at their a priori values, which were constructed from an expanded version of the GEM-T3 tide model [Lerch et al., 1994]; (see Nerem et al. [1993a] for a description of the complete model). The ocean tide model was constructed in the presence of a frequency dependent model of the solid Earth tides developed by Wahr [1981a, 1981b]. While the tidal coefficients were adjusted as ocean tidal terms in the GEM-T3 solution, each parameter which was estimated accommodates ocean, atmospheric and solid Earth mass redistribution at the specified astronomic frequency. For example, the adjustment of the  $S_2(2,2)$  harmonics is used to accommodate the large atmospheric pressure tide in concert with the ocean tides occurring at this frequency. The Wahr solid Earth model has zero for its phase angle and is therefore free of dissipation; however, any residual phase due to anelastic properties of the solid Earth are accounted for in the adjusted ocean tide parameters. The GEM-T3 model contained adjusted terms for the 12 major tidal frequencies and produces error predictions of 2-cm RMS on the radial component of the T/P orbit within a 10-day arc. Therefore the model should accurately reflect the external tidal potential sensed by Earth orbiting satellites arising from the tidal redistribution of mass in the integrated solid Earth-ocean-atmosphere system.

Because of the large number of tidal terms required, an algorithm for efficiently computing all tides within a tidal family is

utilized to reduce the computational burden. Using a formulation developed by O. L. Colombo (unpublished notes and private communications, 1989), these expanded tidal models have been used in the JGM models and are described by *Nerem et al.* [1993a]. Briefly, under the assumption that the admittances of the Earth are sensibly identical at the nearby frequencies within each tidal family, the algorithm takes advantage of the slow modulation of the mainline tides by their sidebands and computes the contribution to the tidal potential of the sidebands through a linear scaling using tidal admittances. This permits efficient computational treatment of the sideband tides. The resulting tide model has over 1600 mainline coefficients being considered, and if one includes the total size of the model considering evaluation of all the terms contained within each of the tidal families, over 6000 terms are being modeled. This is the adopted ocean tide model which is used in the development of the JGM models and the T/P precision orbit determination computations [*Tapley et al.*, this issue].

### Modeling the Rotational Deformation of the Earth

Traditionally, the polar motion of the Earth has been referred to a rather arbitrary conventional international origin (CIO) which nominally conformed to the average pole between the years 1900 to 1905. The earlier GEM models for T/P were developed through the adoption of an Earth-fixed origin based on the observed pole position obtained using SLR tracking data on the LAGEOS satellite between 1979 and 1984. The LAGEOS pole series was used to define a so-called "zero-mean" pole which coincided with the 6-year average of the LAGEOS pole position over this interval. This realization of the terrestrial reference system implied that the mean value of the  $C_{2,1}$ ,  $S_{2,1}$  spherical harmonic coefficients of the geopotential and the mean value of the polar motion  $x, y$  series would be approximately zero. This minimized the impact of unmodeled dynamic polar motion on these gravitational solutions.

With the JGM gravity solutions, we adopted a complete rotational deformation model. This enabled us to utilize the International Earth Rotation Service (IERS) pole series directly as a priori values and to produce gravitational fields consistent with the IERS-adopted CIO origin. A brief discussion of this implementation follows.

The nonrigidity of the Earth is clearly manifested in the temporal variability of its moments of inertia in response to both rotational and tidal deformations. The Earth's axis of figure, which is the principal axis of angular momentum, exhibits two periodic motions. There is daily motion with an amplitude of nearly 60 m due to tidal deformation. The tides are modeled separately (as described above) and are therefore accounted for in the time dependent model of the Earth's gravitational potential. The much smaller motion, with a period similar to that of the Chandlerian and annual wobble, is the Earth's response to rotational deformation. To model this deformation we currently depend on theories [*Lambeck, 1972; McClure, 1973*] which conclude that this deformation is proportional to the main wobbles. The proportionality factor depends on the Earth's elastic properties. It is well known [*Heiskanen and Moritz, 1967*] that the orientation of the axis of figure with respect to some arbitrary frame is reflected in the value of the second degree, order one ( $C_{2,1}$ ,  $S_{2,1}$ ) spherical harmonic in the expansion of the gravitational field. We have employed a general formulation which accounts for the temporal variation of the figure axis through the resulting time dependency of the  $C_{2,1}$ ,  $S_{2,1}$  gravitational terms as follows [*Reigber, 1981*]:

$$\begin{aligned} C_{2,1}(t) &= \bar{C}_{2,1} + K_f \left[ x_p(t) - \{x_p(t_0) + \dot{x}_p \Delta t\} \right] C_{2,0} \sqrt{3} \\ S_{2,1}(t) &= \bar{S}_{2,1} - K_f \left[ y_p(t) - \{y_p(t_0) + \dot{y}_p \Delta t\} \right] C_{2,0} \sqrt{3} \end{aligned} \quad (1)$$

where

$t$	the desired time;
$t_0$	the date for the average pole axis (January 1, 1986 for JGM-2);
$\Delta t$	$t - t_0$ ;
$x_p, y_p$	pole values corresponding to the 6-year average instantaneous rotational axis at the epoch $t_0$ (46.0 and 294.0 milliarcsec in pole x and y coordinates for JGM-2);
$\dot{x}_p, \dot{y}_p$	drift rates for the pole values corresponding to the secular motion of the pole (3.3 and 2.6 milliarcsec/yr in pole x and y);
$\bar{C}_{2,0}, \bar{C}_{2,1}, \bar{S}_{2,1}$	normalized geopotential coefficients, overbars indicate average values;
$K_f$	figure axis scale factor; a value of 0.33 has been adopted based on the ratio of $k_2$ to the so-called secular Love number $k_s$ .

### Modeling of General Relativistic Effects in a Geocentric Frame

The general relativistic effects on a satellite in the geocentric frame [*Ries et al., 1988; Huang et al., 1990; Ries et al., 1991*] are modeled. The general relativistic effects include light time corrections, the Lense-Thirring reference frame drag of a satellite due to the rotating mass of the Earth, geodetic precession, central body effects, and various measurement corrections which depend on the form of the tracking observations (e.g., the number of clocks involved).

### Improved Geodetic Constants

The adopted set of geodetic and reference frame parameters for these solutions, based on Wakker [1990], are reviewed in Table 1. These constants are consistent with those have also been adopted for the T/P precision orbit determination (see *Tapley et al.*, [this issue] for a detailed description of the T/P reference system). Included in this set is an improved LAGEOS-based value of GM ( $398600.4415 \text{ km}^3/\text{s}^2$ ) [*Ries et al., 1992*], the product of the gravitation constant and the Earth's mass, which is consistent with the effects of relativity and a LAGEOS center of mass correction of 25.1 cm.

### Conventional Terrestrial Reference Frame Definition

The kinematic motions of tracking sites are modeled using site positions and velocities based on SLR [*Smith et al., 1990*]. The site velocities default to NUVEL 1 [*DeMets et al., 1990*] where SLR information is unavailable. These coordinates adopted for the SLR sites agree at the few centimeter level with those of the International Terrestrial Reference Frame [*Boucher et al., 1993*] after application of small rotations to put them in identical frames. The kinematic motion of the tracking stations due to ocean loading was implemented and applied to the SLR stations. While the majority of significant station motions are now modeled (including motions arising from plate tectonics, daily resolved Earth rotation and orientation variations, and ocean loading), many smaller effects (e.g., atmospheric loading, few millimeter geocenter motions due to tides) were not included in the JGM models.

**Table 1. Reference Frame and Force Models Utilized in JGM-1 and -2**

	JGM Standard	Reference
<i>Reference Frame</i>		
Conventional Inertial System	J2000	IERS Standards [McCarthy, 1992]
Precession	1976 IAU	IERS Standards
Nutation	1980 IAU	IERS Standards
Planetary Ephemerides	JPL DE-200	IERS Standards
Conventional Terrestrial System	IERS with station positions and site tectonic velocities based on LAGEOS SL7.1 solution or NUVEL 1	Smith et al. [1990] DeMets et al. [1990]
Polar Motion	IERS a priori values: 5-day mean values are adjusted in solutions	IERS Standards
Reference Ellipsoid	$a_e = 6378136.3$ m $1/f = 298.257$ $W_0 = 62636858.702$ m <sup>2</sup> s <sup>-2</sup>	Wakker [1990]
GM	GM = 398600.4415 km <sup>3</sup> s <sup>-2</sup>	Ries et al. [1992]
<i>Force Models</i>		
Rotational Deformation	Time dependent $C_{2,1}, S_{2,1}$	Reigber [1981]
	$\bar{C}_{2,1} = -0.187 \times 10^{-9}$ ( $\bar{x}_p(t_0) = 46$ msec)	
	$\bar{S}_{2,1} = 1.195 \times 10^{-9}$ ( $\bar{y}_p(t_0) = 294$ msec)	
	$\dot{C}_{2,1} = -1.3 \times 10^{-11}/\text{yr}$ ( $\dot{\bar{x}}_p = 3.3$ msec/y)	
	$\dot{S}_{2,1} = 1.1 \times 10^{-11}/\text{yr}$ , ( $\dot{\bar{y}}_p = 2.6$ msec/y)	
	Epoch 1986.0	
Gravity Model	GEM-T3 a priori	Lerch et al. [1993c]
Temporal Gravity	$\dot{J}_2 = -2.6 \times 10^{-11}/\text{yr}$ , Epoch 1986.0	Nerem et al. [1993b]
N Body	DE-200	IERS Standards
Solid Earth Tides	$k_2 = 0.30$ ; $\delta = 0^\circ$ ; $k_3 = 0.093$ with frequency dependence	IERS Standards; Wahr [1981a, 1981b]
Ocean Tides	GEM-T3-based extended model with 90 tide lines	Nerem et al. [1993a]
Relativity	Central Body (Earth)	Ries et al. [1988]
Atmospheric Drag	DTM	Barlier et al. [1987]
Earth Radiation Pressure	Albedo/Infrared	Knocke et al. [1988]

As in all recent GEM models, 5-day average values of Earth orientation parameters (EOP) were adjusted in the JGM models and form an integral part of the terrestrial frame definition. The IERS EOP time series was utilized as the a priori time series. For the later years, this series provides daily values of

polar motion and UT1. Nevertheless, the adjusted JGM time series were 5-day average corrections to the IERS series. The IERS values were not augmented to include rapid (diurnal and semidiurnal) EOP variations due to ocean tides [cf. Brosche et al., 1991; Gross, 1993; Herring and Dong, 1993].

## The JGM-1 Model

### Data Employed

Table 2 shows a summary of the tracking data employed in the JGM-1 model. The data set consists of SLR, TRANET Doppler, DORIS Doppler, and optical tracking data from 31 different satellites, altimeter data from GEOS 3, Seasat, and Geosat, and surface gravity data. The tracking data were essentially processed in the same manner as was done in GEM-

T3 [Lerch *et al.*, 1994], with the addition that along-track one-cycle-per-revolution empirical accelerations were now estimated for some of the lower satellites in order to accommodate nonconservative force model error. Unfortunately, these empirical accelerations also absorb most of the signal arising from the odd zonal gravitational coefficients, thus a similar orbit parameterization must be adopted when using the JGM models for satellites in orbits with similar inclinations/altitudes. The tracking data were rigorously edited in an iterative approach using postprocessing residual analysis. All of the

**Table 2. Orbital Characteristics for Satellites Used in JGM-1 and -2**

Satellite Name	A, km	E	<i>I</i> , degrees	Perigee Height, km	Mean Motion, rev/d	Primary Resonant Period days
ATS-6	41,867	0.001	0.9	35,781	1.01	92.8
Peole	7006	.0162	15.0	515	14.82	2.1
Courier 1B	7469	.0174	28.3	989	13.46	3.8
Vanguard 2	8298	.1648	32.9	562	11.49	2.7
Vanguard 2RB	8496	.1832	32.9	562	11.09	294.3
DI-D	7622	.0842	39.5	589	13.05	8.4
DI-C	7341	.0526	40.0	587	13.81	2.5
BE-C	7507	.0252	41.2	902	13.35	5.6
Telstar 1	9669	.2421	44.8	951	9.13	14.9
Echo 1RB	7966	.0121	47.2	1501	12.21	11.9
Starlette	7331	.020	49.8	785	13.83	2.8
Ajisai	7870	.001	50.0	1487	12.43	3.2
Anna 1B	7501	.0070	51.1	1076	13.37	4.8
GEOS 1	8075	.0725	59.3	1108	11.96	7.0
ETALON 1	25,501	.0007	64.9	19,121	2.13	7.9
TOPEX/POSEIDON	7716	.0004	66.0	1342	12.80	3.2
Transit 4A	7322	.0079	66.8	806	13.85	3.5
Injun 1	7316	.0076	66.8	895	13.87	3.8
Secor 5	8151	.0801	69.2	1140	11.79	3.4
BE-B	7354	.0143	79.7	902	13.76	3.0
OGO 2	7341	.0739	87.4	425	13.79	3.8
OSCAR 14	7448	.003	89.2	1042	13.50	2.2
OSCAR 7	7411	.0242	89.7	848	13.60	3.2
5BN 2	7462	.0058	90.0	1063	13.46	2.4
NOVA	7559	.001	90.0	1123	13.20	6.3
Midas 4	9995	.0121	95.8	1505	8.69	3.0
SPOT 2	7208	.0015	98.7	840	14.17	6.2
GEOS 2	7711	.0308	105.8	1114	12.82	5.7
Seasat	7171	.001	108.0	7171	14.29	3.1
Geosat	7169	.001	108.0	754	14.30	3.0
LAGEOS 1	12,273	.001	109.9	5827	6.39	2.7
GEOS 3	7226	.001	114.9	841	14.13	4.5
OVI 2	8317	.1835	144.3	415	11.45	2.2

tracking and altimeter data were processed uniformly using GSFC's GEODYN orbit determination program, with software verification being provided by the UTOPIA program at University of Texas at Austin/Center for Space Research (UT/CSR) [Tapley *et al.*, this issue].

The GEOS 3, Seasat, and Geosat altimeter data were processed in the form of 15 sec (GEOS 3, Seasat) or 10 sec (Geosat) "normal" points as described by Lerch *et al.* [1994] and Nerem *et al.* [1994b]. A separate distinct ocean dynamic topography model, complete to degree and order 15 in spherical harmonics, was estimated simultaneously with the gravity field for each of the altimeter satellites included in the solution. This was done in order to accommodate any temporal variations in sea level that might occur between the different missions [Nerem *et al.* 1993b]. In addition, an altimeter bias for each satellite was also estimated. The use of satellite altimeter data for simultaneously determining the satellite orbit, the ocean dynamic topography, and the gravity field has been a topic of considerable research [Tapley *et al.*, 1988; Nerem *et al.*, 1990; Marsh *et al.*, 1990b; Denker and Rapp, 1990; Nerem *et al.*, 1994b] and thus will not be further discussed here. Despite the large amount of work which has been done on this subject, there is still concern that long-wavelength oceanography and orbit variations might be correlated, particularly for determining the terms describing the center-of-figure of the dynamic topography, therefore no T/P altimeter data were included in the JGM-2 model which supports the computation of the precise orbit contained on the T/P GDRs.

The surface gravity data were processed in the form of  $1^\circ \times 1^\circ$  mean free-air anomalies created from the data base of Yi and Rapp [1991]. Normal equations were formed from these data as described in detail by Pavlis [1988]. The distribution of the surface gravity data was not completely global, thus predicted gravity anomalies were created to fill in the gaps using a digital terrain model and a topographic/isostatic relationship [Pavlis and Rapp, 1990]. This procedure allowed us to compute gravity solutions without the use of any a priori constraints on the power of the adjusted coefficients.

### Solution Methodology

Given the elimination of the a priori coefficient constraints used in previous T/P-era gravity models, the JGM models were produced using a classic weighted least squares procedure. Each of the data sets listed in Table 2 were used to compute a set of least squares normal equations containing the partial derivatives of the observations with respect to each of the estimated parameters in the solution. GSFC's SOLVE linear system software was used to combine each of these normal equations in order to compute the final gravity solution. The SOLVE program is also used in the calibration and optimization of the models. Numerous solutions using different data weights, different combinations of data subsets, and different sets of adjusting parameters are all routinely inverted using SOLVE. The JGM modeling efforts have been in the forefront of developing calibration and optimal data weighting techniques to enable systematic errors in specific data sets to be better understood [Lerch, 1991; Lerch *et al.*, 1985, 1991, 1993a]. The calibration technique essentially consists of computing a series of gravity solutions with each major data set removed in one of the "subset" solutions. The difference of the coefficients for each subset solution compared to the full solution is then compared to the difference in the errors predicted

by the error covariance of the solutions. Data weights were iteratively adjusted until the condition is satisfied that the expected mean square deviation of all subset solutions from the full solution's values are predicted by the solutions' error covariances [cf. Lerch *et al.*, 1993a]. Numerous independent tests [Lerch *et al.*, 1993a] have indicated that this method of calibration results in very reliable error estimates for the resulting gravity model.

The weights given to each major data set are given in Table 3. LAGEOS and Starlette received the greatest weight in the solution, but even these data are weighted much less than the precision of the tracking data. The current need to downweight the data (to get a realistic solution error covariance) and the systematic trends in the a posteriori laser residuals both indicate that there is significant unmodeled signal in the data. There is clearly a large loss in our processing of these observations which could be avoided if improved supporting models and a better understanding of the physical processes involved could be applied. Experiments have been performed where the Starlette laser data in the solution have been given an increased weight by a factor of 100. The resulting model showed virtually no improvement in its ability to fit the Starlette laser data when compared to JGM-2; this strongly indicates that most of the remaining signal seen within the residuals is attributable to either currently unmodeled sources such as temporal variations in gravity, and/or errors in nongravitational force and measurement models. Increasing the size of the adjusted gravity model also yields little improvement in data fit. Therefore truncation errors in the modeling of the static field are not the source of these problems. Improved modeling of nonconservative forces and nontidal temporal variations in gravity (cf. Nerem *et al.* [1993b]; Chao and Eanes [1994]) are likely major sources of unaccommodated effects and clearly warrant further studies.

The data weighting of the surface gravimetry entailed a two-step process. First, the formal measurement accuracy assigned to each  $30' \times 30'$  free-air anomaly block was calibrated with respect to a gravity model based only on satellite tracking data [Pavlis, 1988]. This process yielded gravity anomaly uncertainties of between 8 and 16 mGal within observed regions. The isostatically predicted anomalies based on topographic/bathymetric data received somewhat higher uncertainties. These anomalies were then used in combination to form normal equations and combined with other data forming JGM-1. Further calibration tests yielded a scaling weight of 0.25 for the surface gravity data. The down weighting of the surface gravity data was necessary because the performance of the gravity model for satellite orbit determination degraded when the data received a higher weight. This type of behavior is indicative of unmodeled errors present in the gravity data. There was some suspicion that long-wavelength errors in the surface gravity data might be creating the problem. In order to alleviate this problem, the surface gravity data were not allowed to contribute to gravity coefficients lower than degree and order 5. Instead, a separate  $5 \times 5$  gravity model was estimated simultaneously with JGM-1 for which only the surface gravity data contributed. While this procedure did allow the surface gravity data to be included in the JGM models with strong weight, the solution to the problem also undoubtedly weakened the final gravity model by eliminating useful gravity signal, thus a better understanding of this problem is needed for future models. Possible variable weighting of the normal equations associated with different parameters should be investigated for certain data types such as surface gravity data.

**Table 3a. Summary of Data Used in JGM-1 and -2**

Data Set	Data Type	Number of Observations	Number of Arcs	Weights $\sigma'_o$ , cm
GEOS 3:ATS	Laser	16,935	26	408
GEOS 3:ATS	SST	27,400	26	0.8 <sup>+</sup>
Peole	Laser	4315	6	632
DI-D	Laser	11,607	6	632
DI-C	Laser	7680	4	408
BE-C	Laser	64,827	39	277
Starlette	Laser	207,454	171	169
Ajisai	Laser	257,546	49	223
GEOS 1	Laser	114,338	60	353
Etalon 1	Laser	2918	4	85
TOPEX/POSEIDON*	Laser	49,847	15	156
TOPEX/POSEIDON*	DORIS	748,117	14	0.98 <sup>+</sup>
Oscar 14	Doppler	62,277	13	14.1 <sup>+</sup>
Nova	Doppler	72,954	16	1.8 <sup>+</sup>
SPOT 2	DORIS	429,073	32	0.7 <sup>+</sup>
GEOS 2	Laser	18,847	23	447
Seasat	Laser	13,018	14	707
Seasat	Doppler	123,516	14	3.2 <sup>+</sup>
Seasat	Altimeter	92,462	14	353
Geosat	Doppler	555,668	13	2.0 <sup>+</sup>
Geosat	Altimeter	275,239	13	353
LAGEOS 1980-1988	Laser	434,729	108	112
LAGEOS 1992-1993*	Laser	61,175	14	158
GEOS 3	Laser	76,662	61	158
GEOS 3	Laser+Altimeter	200,862	69	577
Optical (20 sats)	Optical	201,429	496	
Surface Gravity		64,800	1	

\* Data not present in JGM-1

+ Weights in centimeters per second

### Solutions Developed

The JGM-1 model is complete to degree 70 in spherical harmonics and represents the final prelaunch model for T/P precision orbit determination. In addition, we have created the JGM-1S gravity model which contains only the satellite tracking data included in JGM-1. This model was developed for investigators who desire a model determined solely from satellite orbit perturbations. JGM-1S is complete to degree 60, and was obtained using a priori constraints which minimized the power of the coefficients as was done in previous models [Lerch *et al.*, 1993b].

The three ocean dynamic topography models for GEOS 3, Seasat, and Geosat estimated in the JGM-1 model are quite

similar to the models computed in GEM-T3 [Lerch *et al.*, 1994; Nerem *et al.*, 1994b] and thus will not be extensively discussed here. In brief, considering the error estimates for the dynamic topography solutions and corresponding oceanographic data, the JGM-1 models compare well to similar models computed from historical oceanographic data [Levitus, 1982]. However, all of the historical altimeter data suffer from a lack of supporting environmental corrections (ionosphere, troposphere, etc.). Furthermore, ocean tidal uncertainties and their long aliasing periods (e.g.,  $S_2$  has a ~360-day aliasing period for Geosat) caused systematic errors in the recovered dynamic topography models obtained from JGM-1/-2. However, with T/P, much more refined models are routinely being obtained [Nerem *et*

Table 3b. Summary of Optical Data Used in JGM-1 and -2

Data Set	Number of Observations	Number of Arcs	Weights $\sigma'_o$ , Arcsec
Courier 1B	2470	10	6.7
Vanguard 2	1290	10	6.7
Vanguard 2RB	681	10	6.7
DI-D	6032	9	9.4
DI-C	2692	10	9.4
BE-C	7505	50	9.4
Telstar 1	3946	30	8.2
Echo 1RB	4468	32	9.4
Anna 1B	4043	28	8.2
GEOS 1	60,737	43	11.5
Transit 4A	3831	50	9.4
Injun 1	3264	44	9.4
Secor 5	721	13	6.7
BE-B	1734	20	6.7
OGO 2	1204	16	6.7
Oscar 7	1851	4	6.7
5BN 2	818	17	8.2
Midas 4	31,749	50	9.4
GEOS 2	61,431	46	11.5
OVI 2	962	4	6.7

*al.*, this issue], due in large part to improved altimeter measurement modeling, improvements in the ocean tide model, and much more accurate orbit positioning.

For the JGM-1/-2 dynamic topography models, the difference of the Seasat and Geosat models clearly shows the presence of the El Niño episode during the early part of the Geosat mission [Nerem *et al.*, 1994b]; this demonstrates the importance of estimating separate dynamic topography models for each discrete time period covered by a particular mission.

We put off the discussion of the evaluation of this gravity model until later in the paper when both JGM-1 and 2 can be discussed together. As will be discussed, the error covariance for JGM-1 indicates that gravity-induced errors on T/P should be less than 4 cm RMS radially. Provided that the JGM-1 error covariance is realistic, the gravity model accuracy objective for T/P was far surpassed by this prelaunch model. This was clearly an exciting result; the arrival of actual T/P tracking data allowed further improvement and extensive orbit accuracy assessments confirming this performance estimate.

### JGM-2 Model Development

The final step in developing the gravity model used for T/P precision orbit computations was to add T/P SLR and DORIS tracking data to the JGM-1 model. This was necessary to further improve the JGM-1 model, particularly for the gravity coefficients that are most T/P specific, the resonant coefficients

and low degree and order coefficients having strong m-daily perturbations. The schedule called for a tuned gravity model to be completed within 6 months of the beginning of the T/P mission, thus only a limited time period of SLR and DORIS tracking data could be considered for inclusion in the model. Early analysis of the T/P tracking data using the JGM-1 gravity model provided two crucial pieces of information: (1) the T/P orbit determination accuracy was roughly at the level predicted by the JGM-1 covariance, and (2) T/P was experiencing forces of a nonconservative nature which were not predicted by any of the prelaunch spacecraft models [Marshall and Luthcke, 1994; Nerem *et al.*, 1993a]. While the performance of JGM-1 was encouraging, the errors in the nonconservative force models were at least as large as the remaining gravity model errors, thus the tuning of the JGM-1 gravity model with T/P tracking data sought to improve both the gravity model and the nonconservative force models simultaneously. This complicated the computation of the final T/P postlaunch gravity model more than anticipated, and to our knowledge, this was the first time a satellite surface force model was evaluated and improved in this way. These activities will now be discussed in detail.

### Processing of TOPEX/POSEIDON Data

Due to the time constraints mentioned above, the analysis of T/P tracking data was limited to the first 148 days of the mission (cycles 1-15, September 25, 1992 to February 18, 1993). The SLR and DORIS station coordinates adopted for this anal-

ysis were from UT/CSR [Eanes and Watkins, 1993; Watkins et al., 1992] to be compatible with our adopted polar motion time series also produced at UT/CSR. The data were processed in fifteen 10-day arcs, each encompassing one of the T/P mission cycles. For each arc, the estimated parameters included the satellite position and velocity at arc epoch, a daily drag coefficient, a single solar radiation pressure coefficient, daily one cycle-per-revolution (1 CPR) empirical accelerations in the along-track and normal directions, frequency biases and troposphere scale parameters for each pass of the DORIS data, and a time bias for the DORIS network relative to the SLR network. Using this parameterization and the JGM-1 gravity model, fits to the SLR and DORIS data of 5-6 cm and 0.56 mm/s RMS, respectively, were routinely achieved. These orbits were then used to construct least squares normal equations containing the partial derivatives of the observations with respect to the estimated parameters, which included the orbit parameters listed above, as well as parameters describing each plate of the box-wing nonconservative force model, the 70 x 70 gravity field, station coordinates, and polar motion. Within the gravity solution, the 1 CPR parameters were linearly shifted and constrained to zero (i.e., using the normal matrix, all the right-hand side values were linearly scaled to account for fixing these parameters as though they were not adjusted and had values of zero) in order to force reduction of the residual signal by physical model parameters apart from these strictly empirical terms. The residual 1 CPR signal not absorbed by the box-wing model or the gravity model was not found to have a deleterious effect on the solution at any detectable level; nevertheless, it was found that the box-wing model accounted for ~95% of the thermal and radiative forces acting on T/P as is described below.

The normal equations for the T/P SLR and DORIS data were combined with the JGM-1 normal equations. The weight assigned to the SLR and DORIS data was individually determined using the subset solution calibration technique discussed earlier while holding the JGM-1 data weights fixed. Since polar motion parameters are estimated simultaneously in the gravity solution, it was necessary to process and include LAGEOS SLR data during the T/P time frame in order to better define the reference frame over that which could be done with T/P alone. The addition of T/P and LAGEOS normal equations represent the only data differences between JGM-1 and JGM-2. Since an extensive set of earlier LAGEOS data was already included in the JGM-1 model, differences between the JGM-1 and -2 models can be attributed almost entirely to the addition of T/P tracking data.

#### Tuning of the T/P Box-Wing Model

Until recently, gravity field mismodeling was the major source of error in precise orbit determination. However, with improvements in these models, accurate modeling of the non-conservative forces on T/P have become a significant concern [Marshall and Luthcke, 1994; Ries et al., 1993]. In order to achieve the T/P orbit determination goals, it was no longer prudent to ignore the rotating, attitude controlled, geometrically complex shape of T/P. Therefore the "box-wing" representation, which treats the spacecraft as a combination of flat plates arranged in the shape of a box and a connected solar array, was developed [Marshall and Luthcke, 1994]. The nonconservative forces acting on each of the eight surfaces are computed independently, yielding vector accelerations which are summed to compute the total aggregate effect on the satellite

center-of-mass. Parameters associated with each flat plate were derived from a finite element analysis of the T/P spacecraft [Antreasian and Rosborough, 1992]. Certain parameters can be satisfactorily inferred from tracking data and have been adjusted to obtain a better representation of the satellite acceleration history. Changes in the nominal mission profile and the presence of an on-orbit "anomalous" force complicated this tuning process.

The eight flat plates used in the approximation consist of six for the box and one each for the front and back of the solar array. The following parameters are associated with each plate in the box-wing model: area, specular reflectivity, diffuse reflectivity, emissivity, cold equilibrium temperature, temperature differential between hot and cold equilibrium temperature, exponential decay time for panel cooling, exponential decay time for panel heating, and temperature/satellite rotation scale factor. A priori values for these parameters were obtained through a least squares fit of each force model (solar, thermal imbalance, Earth albedo and IR) to the accelerations derived through elaborate finite element analysis [Antreasian and Rosborough, 1992]. The pertinent acceleration equations and a summary of this process can be found by Marshall and Luthcke [1994]. Modeling the spacecraft attitude is intrinsic to the box-wing model. The Sun-Earth-T/P orbit geometry is represented by two angles:  $\beta'$ , which refers to the angle between the Sun vector and the orbit plane, and the orbit angle  $\Omega$ , which is measured from the inertial coordinate system  $Y$  axis. The T/P attitude control laws vary depending upon the  $\beta'$  and  $\Omega$  regime as described by Marshall and Luthcke [1994]. The attitude of T/P is modeled in the GEODYN orbit determination software and checked against spacecraft telemetry in order to ensure that the spacecraft is performing as predicted.

Just as the gravity field benefits from the addition of actual T/P tracking data, the "box-wing" model can be improved using actual tracking data. In addition, the impact of aliasing of errors in the box-wing parameters into the gravity model when tuning has been examined. The GSFC ERODYN error analysis package [Englar et al., 1978] was used to perform a consider analysis in which errors in the box-wing parameters were propagated into the recovered geopotential coefficients. The intent was to identify that portion of the geopotential model which has a similar signal on the T/P orbit as that arising from the box-wing parameters and assess box-wing error contribution if unadjusted during the gravity tuning effort. In order to apply realistic, and perhaps pessimistic, error bounds for the box-wing model, information on spacecraft material properties were obtained from O'Donnel and Whitt [1992] and O'Donnel et al. [1991]. The following initial errors were considered: 100% of the calibrated JGM-1 covariance, box-wing model; area, 0.5 m<sup>2</sup> for the box and 0.1 m<sup>2</sup> for the solar array; specular reflectivity, 0.3 for the box and 0.1 for the solar array; diffuse reflectivity, 0.3 for the box and 0.1 for the solar array; and emissivity, 0.1 for all surfaces. SLR and DORIS T/P tracking data from cycles 1-4 were reduced into normal equations and used for this study. The consider parameter set included the surface cross-sectional area, specular and diffuse reflectivities, and emissivities for all eight plates.

The degree and order variances of the box-wing errors aliased into the tuned gravitational field were computed as a percentage of the calibrated JGM-1 1 $\sigma$  coefficient uncertainties. The box-wing parameters cause a nonconservative force mismodeling which induces a predominantly 1 CPR orbit error. In terms of spherical harmonic coefficients, the 13, 15

and 17th degrees and the 12, 25, and 38th orders are most affected, with changes as large as 40% of JGM-1's error estimates being observed. The odd zonals were also very much affected, with changes as large as 10% of the JGM-1 uncertainty. Clearly, the accuracy with which these coefficients could be recovered in JGM-2 depended on the errors in the prelaunch box-wing model, since it was difficult to separate these signals in the gravity solution.

The daily residual along-track accelerations determined from orbital fits to the T/P SLR and DORIS tracking data using the prelaunch box-wing model are shown in Figure 1. These values represent the daily average difference between the predicted box-wing along-track accelerations and the actual accelerations measured on T/P. The unmodeled acceleration is usually less than  $1 \text{ nm/s}^2$  in magnitude. Presumably, these differences arise principally from deficiencies in the box-wing model. Since this signal was not observed in the prelaunch analysis, it is reasonable to assume that the finite element model did not predict this spacecraft behavior. Thus the force is termed "anomalous." Nevertheless, the prelaunch box-wing model accounts for over 95% of the observed acceleration acting on the spacecraft. Examination of Figure 1 reveals the magnitude of the anomalous force is nearly the same at recurring spacecraft-Sun-Earth geometries. Furthermore, the force behavior is consistent with a body-fixed force directed along both the positive  $X$  and  $Y$  spacecraft axes. Although the anomalous force behaves like a body-fixed  $X$  and  $Y$  acceleration, its source remains elusive.

The box-wing parameters were estimated simultaneously in the JGM-2 gravity solution in order to improve the prelaunch values. The process followed the same methodology as used

in the simulations to determine the best set of box-wing parameters for adjustment [Luthcke and Marshall, 1992]. The additional effect of Earth radiation mismodeling, the change in solar array pitch bias, the addition of near global DORIS tracking data, and the combination of data from all  $\beta'$  regions produced a different solution environment than used in the prelaunch simulations. However, the overall parameter set did not require substantial change from that derived in the simulations. The biggest change was to the adjustment of the plate cross-sectional areas in that opposite plates were tied to adjust together. Correlation problems with the drag terms required that some of the parameters be slightly constrained.

Body-fixed  $X_a$  and  $Y_a$  empirical forces were introduced into the model in an attempt to properly account for the anomalous force. However, these terms were highly correlated with many of the box-wing parameters. Also, the deep resonant orders of the geopotential experienced large changes in this tuning process since they absorb much of the nonconservative force modeling errors not accommodated by the body-fixed accelerations. Consequently, the values for the  $X_a$  and  $Y_a$  accelerations were determined independently of the box-wing, gravity, and drag terms, resulting in realistic values of  $X_a = 0.39 \text{ nm/s}^2$  and  $Y_a = 0.20 \text{ nm/s}^2$ . These accelerations were used as fixed a priori values and the gravity field and box-wing models were tuned appropriately. Figure 1 shows that the resulting residual along-track accelerations have been substantially reduced after tuning. The spikes during the spacecraft yaw flips in cycles 6 (day 57) and 11 (day 106) have been virtually eliminated. Even more telling is the reduction in the recovered amplitude of the 1-CPR acceleration parameters over the same period displayed in Figure 2. These give a more independent

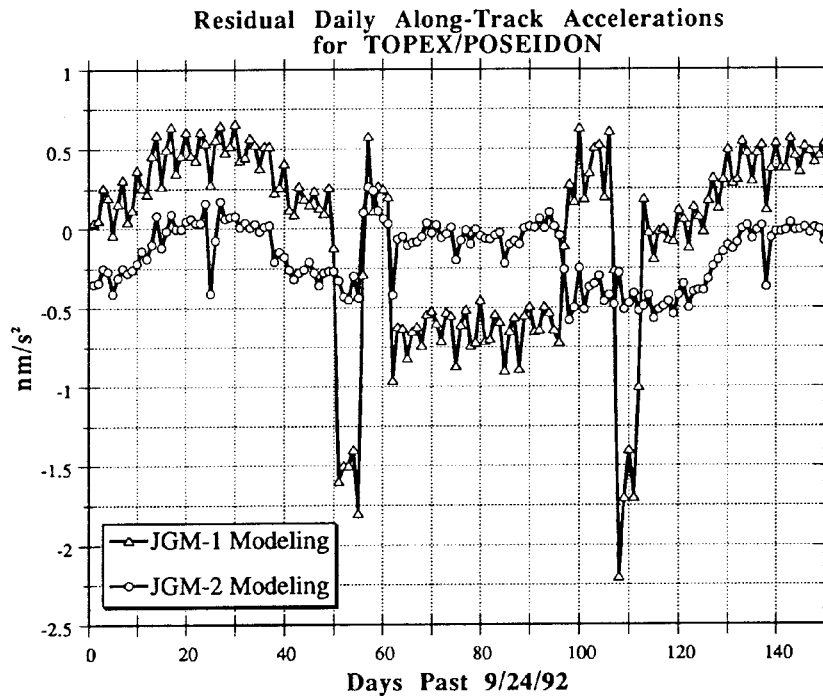


**Figure 1.** Daily values of residual along-track accelerations for TOPEX/POSEIDON using the prelaunch and postlaunch gravity and box-wing models.

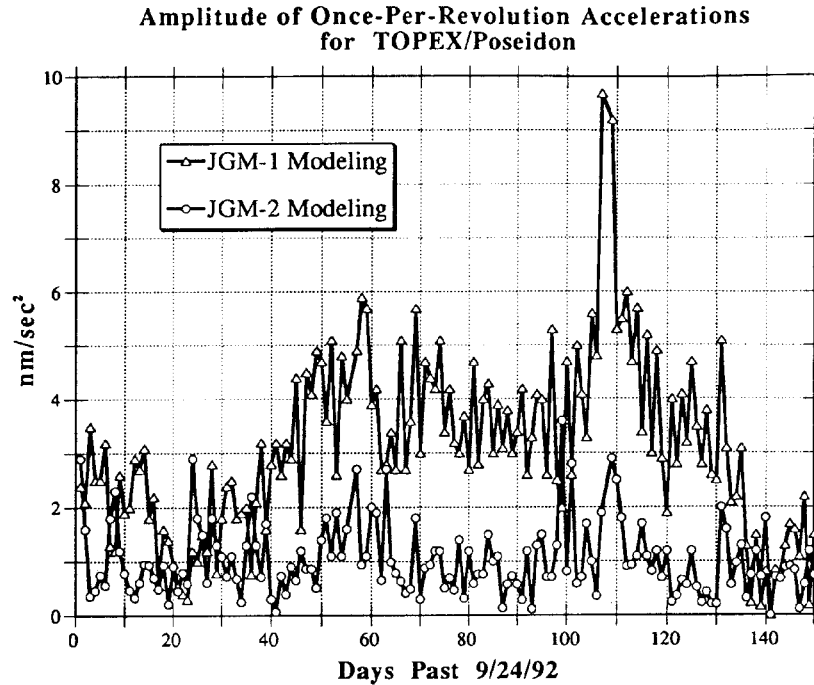


**Figure 2.** Daily amplitude of the 1-CPR along-track accelerations for TOPEX/POSEIDON using the pre-launch and postlaunch gravity and box-wing models.

measure of the macromodel performance since they are not as correlated with the applied  $X_a$  and  $Y_a$  constant body-fixed accelerations.

#### Solutions Developed

Three models have been developed which share the JGM-2 "heritage." JGM-2 is the final postlaunch model for T/P and is used in the computation of orbit for the T/P GDRs [Tapley *et al.*, this issue]. JGM-2S contains only the satellite tracking data used in JGM-2 and is thus its "satellite-only" equivalent. JGM-2S is complete to degree 70 and was constrained using the same technique as described for JGM-1S earlier. In order to accommodate geophysicists who cannot use models which contain topographically predicted gravity information, we have also constructed JGM-2G which differs with JGM-2 only in that the topographically predicted anomalies included in the surface gravity normal equations were replaced with anomalies computed from JGM-2S. Because of the a priori constraints employed in JGM-2S, this has the effect of setting the short wavelength gravity to zero at the locations lacking surface gravimetry; however, we now believe that this is a superior approach to biasing the whole model toward zero as is done with the a priori constraint approach used in the GEM-T3 and GEM-T3A models [Lerch *et al.*, 1994; Nerem *et al.*, 1994a].

The coefficients of the JGM-2 model and their  $1\sigma$  errors are given in Table 4 to degree and order 9. The errors given in Table 4 should be interpreted with caution, especially for the higher degree terms and the zonal coefficients, since many of the coefficients have highly correlated errors. The complete JGM-2 model, and any of the other models discussed in this paper, are available via anonymous ftp (file transfer protocol) on the science internet at [geodesy.gsfc.nasa.gov](ftp://geodesy.gsfc.nasa.gov).

#### Evaluation of the Models

##### Characterization of the Models and Their Errors Versus Degree

Since the satellite tracking data mainly contribute to the lower degree coefficients and the altimeter and surface gravity data mainly to the higher degree terms, an evaluation of the characteristics of the model coefficients and their errors versus degree can be helpful. Figure 3 shows the degree variance of JGM-2 compared to the GEM-T3 and OSU91A models (JGM-1 is nearly identical to JGM-2 and thus not shown). What this figure clearly demonstrates is the deleterious effect that the use of a priori constraints via Kaula's Rule had on the recovered power of the GEM-T3 gravity model. From degrees 25 to 50, the power of the GEM-T3 model is well below that of OSU91A and JGM-2, neither of which employed any a priori constraints. GEM-T3 contains most of the same data as JGM-2, yet the a priori constraints have clearly dampened the model at high degrees. The a priori constraints were required in the GEM-T3 solution since the altimeter and surface gravity data did not provide complete global coverage. However, with the introduction of topographically predicted anomalies in JGM-2 (or satellite-based anomalies in JGM-2G) to fill in the coverage gaps in the altimeter and surface gravity data, the a priori constraints may be removed since the "singularities" in the solution will have been eliminated via the "fill-in" anomalies. The low power of JGM-2S is also caused by the application of the a priori constraints; this is necessary since the satellite tracking data cannot separate many of the high-degree coefficients from each other, and constraining their power seems to provide stable solutions.

**Table 4. JGM-2 Coefficients and Errors to Degree 9 Fully Normalized**

$l$	$m$	$C_{lm}$	$S_{lm}$	$\sigma C_{lm}$	$\sigma S_{lm}$
2	0	-484.1654663 †		0.0001090	
2	1	-0.0001870	0.0011953		
2	2	2.4390838	-1.4001093	0.0001240	0.0001240
3	0	0.9571224		0.0000261	
3	1	2.0283997	0.2488066	0.0004170	0.0004160
3	2	0.9044086	-0.6192306	0.0002660	0.0002920
3	3	0.7211539	1.4140369	0.0002010	0.0001970
4	0	0.5401433		0.0002600	
4	1	-0.5363680	-0.4734226	0.0002350	0.0002280
4	2	0.3503493	0.6628689	0.0004270	0.0004390
4	3	0.9902582	-0.2010099	0.0002290	0.0002210
4	4	-0.1884885	0.3088453	0.0002100	0.0002120
5	0	0.0684645		0.0001570	
5	1	-0.0591214	-0.0955327	0.0008440	0.0008490
5	2	0.6533875	-0.3237786	0.0006760	0.0007060
5	3	-0.4519017	-0.2150966	0.0003910	0.0003840
5	4	-0.2950801	0.0496700	0.0002510	0.0002450
5	5	0.1749710	-0.6696502	0.0002490	0.0002480
6	0	-0.1500030		0.0003540	
6	1	-0.0761294	0.0265588	0.0004870	0.0004880
6	2	0.0486483	-0.3737880	0.0008020	0.0008380
6	3	0.0579537	0.0090304	0.0006450	0.0006160
6	4	-0.0862993	-0.4716700	0.0003700	0.0003710
6	5	-0.2671890	-0.5365234	0.0001980	0.0002000
6	6	0.0098855	-0.2370946	0.0002440	0.0002460
7	0	0.0909460		0.0003620	
7	1	0.2758256	0.0967770	0.0012000	0.0011800
7	2	0.3278766	0.0940337	0.0012400	0.0012700
7	3	0.2508965	-0.2166254	0.0008340	0.0008390
7	4	-0.2755462	-0.1238634	0.0005470	0.0005310
7	5	0.0018128	0.0177164	0.0003580	0.0003680
7	6	-0.3590382	0.1517702	0.0001630	0.0001630
7	7	0.0012547	0.0244337	0.0003130	0.0003090
8	0	0.0493049		0.0005210	
8	1	0.0232834	0.0591996	0.0009020	0.0008910
8	2	0.0787560	0.0662488	0.0011400	0.0012100
8	3	-0.0208114	-0.0866613	0.0011500	0.0010900
8	4	-0.2448369	0.0702875	0.0007900	0.0007880
8	5	-0.0251488	0.0892490	0.0004520	0.0004490
8	6	-0.0651558	0.3092402	0.0003520	0.0003460
8	7	0.0671575	0.0746269	0.0002030	0.0002070
8	8	-0.1238923	0.1204626	0.0003820	0.0003880
9	0	0.0267036		0.0005730	
9	1	0.1462664	0.0206503	0.0013500	0.0012700
9	2	0.0245294	-0.0337777	0.0016000	0.0015900
9	3	-0.1619243	-0.0751423	0.0013200	0.0013300
9	4	-0.0085254	0.0192064	0.0010100	0.0009880
9	5	-0.0166623	-0.0543111	0.0007230	0.0007310
9	6	0.0626750	0.2224258	0.0004600	0.0004740
9	7	-0.1184886	-0.0965854	0.0003780	0.0003690
9	8	0.1884251	-0.0031477	0.0002840	0.0002840
9	9	-0.0481248	0.0966002	0.0004780	0.0004750

Units of  $10^{-6}$ . The complete JGM-2 model to degree 70, as well as other models discussed in this paper, are available via anonymous ftp from [geodesy.gsfc.nasa.gov](http://geodesy.gsfc.nasa.gov).

† Permanent deformation not included.

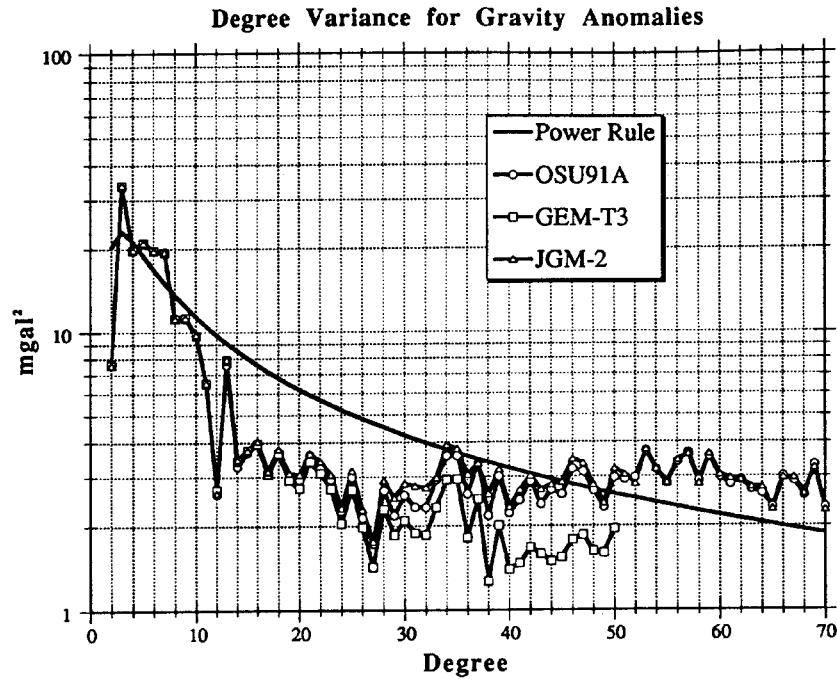


Figure 3. Gravity anomaly degree variance for different gravitational models.

Figure 4 shows the RMS coefficient error by degree for JGM-2, GEM-T3A, and GEM-T3 as computed from their calibrated error covariances (JGM-1 is nearly identical to JGM-2 and thus not shown). The benefit of the combination solutions over a satellite-only solution such as JGM-2S is clearly demonstrated. In addition, the inclusion of SPOT 2 DORIS track-

ing data in GEM-T3A versus GEM-T3 demonstrates the importance of this data type [Nerem et al., 1994a]. The improvement of JGM-2 over GEM-T3A is also interesting since these two models contain basically the same data. The difference is attributed to the improvement in processing techniques, background models, reference frame, etc., which were

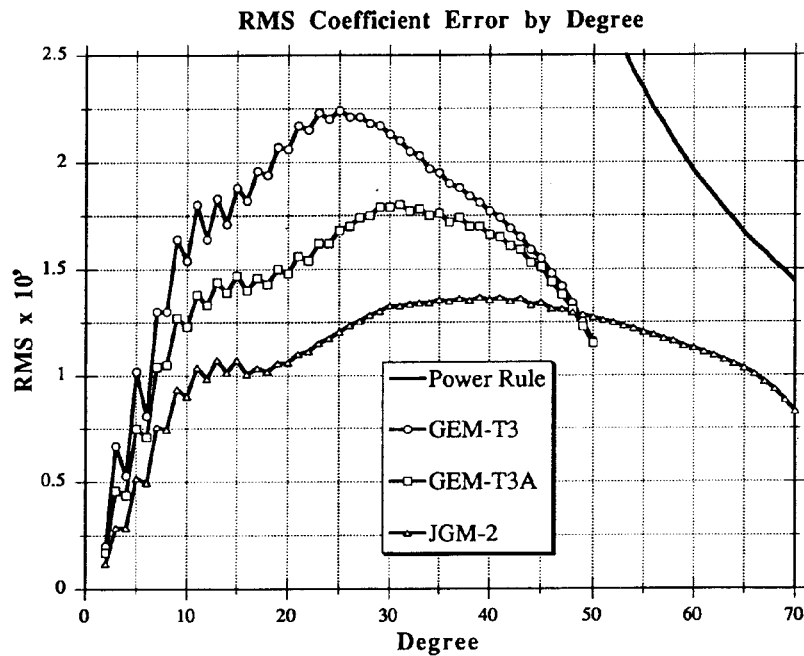


Figure 4. Coefficient degree error variance for different gravitational models.

adopted for the development of the JGM-2 model. The improvement of JGM-2 over JGM-1 was primarily for the T/P-sensitive resonant coefficients (orders 12, 25, and 38) and the coefficients of order 1 and 2. The improvement of the order 1 coefficients was particularly important since they caused much of the geographically correlated orbit error for T/P observed in JGM-1 [Christensen *et al.*, 1994].

#### Predicted Orbit Accuracy Assessment for TOPEX/POSEIDON

The predicted performance on T/P using different gravity models can be assessed using the error covariance of each model. The mapping of gravity coefficient variations into orbit errors was accomplished by Kaula [1966] and later extended by Rosborough [1986], Rosborough and Kelecy [1990] to include the variation with geographic location. These relations can be used to map the gravity model error covariance into satellite orbit errors and their variation with latitude and longitude. Table 5 gives a summary of the RMS radial, cross-track, and along-track orbit errors for T/P using different gravity models. The improvement in the predicted performance of the gravity models for T/P from GEM-T1 to JGM-2 is striking. Clearly, the 2-cm performance of JGM-2 on T/P far surpasses the 10-cm mission requirement if the error covariance matrix is realistic. This performance for JGM-2 is a result of nearly a decade of work achieved through the improvement of solution, data quality, and orbit determination techniques.

Figure 5 shows the predicted radial orbit error ( $1\sigma$ ) using the JGM-1 and -2 error covariances as a function of orbit inclination for a satellite at the altitude of T/P. The reduction of the radial orbit error at the  $66^\circ$  inclination of T/P and its complement ( $114^\circ$ ) for JGM-2 versus JGM-1 is apparent, although the benefit of the T/P tracking data in JGM-2 is not seen for inclinations significantly different from  $66^\circ$ . The radial orbit error increases for orbital inclinations closer to the equator because of a lack of suitable low inclination tracking data in the JGM-2 model. However, for orbit inclinations closer to the poles, the performance of T/P is not severely degraded from the nominal  $66^\circ$ . Clearly, JGM-2 could provide T/P radial orbit error performance for other inclinations at the same altitude, especially if tracking data at these inclinations were used to further improve the model.

Plate 1 shows the predicted radial orbit error for the average of the ascending and descending tracks computed as a function of geographic location using the error covariances of JGM-1 and -2 [Rosborough, 1986; Rosborough and Kelecy, 1990]. Herein, the geographically correlated component of the radial orbit error is defined as the average error for the ascending and descending tracks at each geographic location, since the error will average into a determination of the mean sea surface in this manner. The geographically correlated errors for JGM-1 have an RMS of 2.6 cm and are always less than 3.5 cm. For JGM-2, the geographically correlated orbit error is less than 2.2 cm at all locations, with a global RMS of 1.6 cm. Comparisons to independent orbits computed using T/P GPS tracking data have shown differences which are reminiscent of the error predictions shown here [Christensen *et al.*, 1994], suggesting that some further improvements in JGM-2 for T/P might be realized. There has clearly been a reduction in the geographically correlated component of the radial orbit error for JGM-2 over JGM-1, but there is also some geographically correlated error still remaining due to the historical distribution of tracking data contained in the JGM models and gaps in coverage for the T/P SLR and DORIS tracking data. The continuous tracking provided by the GPS receiver on T/P should eliminate the small remaining error for T/P seen in JGM-2 [Christensen *et al.*, 1994; Schutz *et al.*, 1994]. In addition, we have seen evidence that the addition of more T/P SLR/DORIS tracking to the solution (tripling the amount of T/P data in the JGM-2 model) can also nearly eliminate the remaining error.

#### Performance for TOPEX/POSEIDON

Tapley *et al.* [this issue] summarize the precision orbit determination accuracy for T/P as a whole (using the JGM-2 gravity model), thus our purpose here is to evaluate the performance of the JGM-2 model versus previous models. The performance of a gravity model for T/P precision orbit determination is uniform in time due to its 10-day repeating ground track, so we have chosen a single 10-day arc on which to base our evaluations. Since tracking data from cycles 1-15 were included in the development of JGM-2, we have chosen a time period after these initial 150 days in order to get a more independent evaluation of the performance of the models.

Cycle 32 (July 27 to August 6, 1993) was chosen as the test

**Table 5. Predicted Orbit Error Due to Gravity for TOPEX/POSEIDON**

Gravity Model	Radial	Cross-Track	Along-Track
GEM-L2	65.4	73.5	262.5
GEM-T1	25.0	31.1	222.1
GEM-T2	10.21	15.5	145.7
GEM-T3S	12.8	19.4	175.2
JGM-1S	6.0	8.7	97.6
JGM-2S	2.9	5.6	58.0
GEM-T3	6.8	12.2	122.0
GEM-T3A	5.0	8.6	92.3
JGM-1	3.4	6.0	65.5
JGM-2	2.2	4.0	35.9

Zonal errors not included. Units in centimeters.

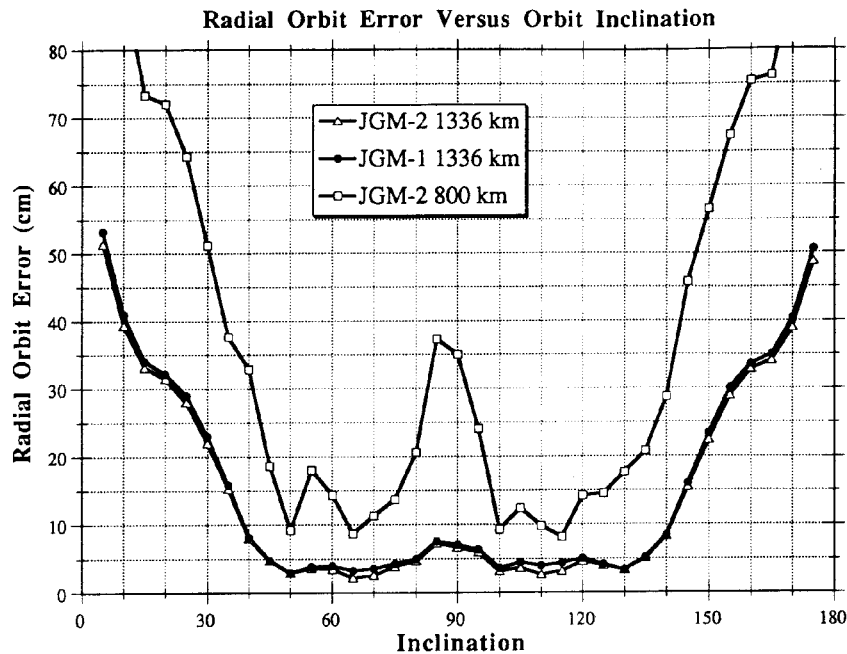


**Figure 5.** Predicted radial orbit error for TOPEX/POSEIDON and ERS 1 using the error covariance matrix of the gravity model.

case because the satellite experiences no maneuvers during this time period and good tracking coverage was obtained by the SLR, DORIS, and GPS tracking systems. Using a variety of historical gravity models, the SLR and DORIS tracking data for cycle 32 were used to determine the orbit of T/P using identical models for ocean tides, nonconservative forces, station coordinates, etc. The RMS of the SLR and DORIS tracking data residuals, which are the difference between the actual observations and the modeled observations, are shown in Table 6, along with the computed altimeter crossover differences and RMS altimeter residuals. The reduction of gravity model errors for T/P orbit determination over the history of the T/P development activity is evident. Table 7 shows the difference between each of these orbits and the orbit computed by the Jet Propulsion Laboratory using the GPS tracking data and their "reduced-dynamic" orbit determination technique [Bertiger *et al.*, this issue; Yunck *et al.*, 1994]. The GPS orbit was computed using the JGM-2 gravity model and thus it has some advantage over the orbits computed using older models. However, the technique is less sensitive to dynamic model errors than the more dynamic technique employed in this paper, thus the GPS reduced-dynamic orbits can provide a somewhat independent comparison to the more dynamically dependent SLR/DORIS orbits. Again, the improvements in the gravity model performance for T/P from GEM-L2 to JGM-2 is striking. Tables 5 and 7 show that the radial orbit errors implied by the orbit differences are well predicted by the error covariances of the gravity solutions, with the exception of GEM-T2 which was known to have an optimistic error covariance. The along-track orbit differences are much smaller than predicted by the covariance analysis because of the 1-CPR accelerations estimated in the orbit fits absorbed some of the along-track orbit error caused by gravity mismodeling.

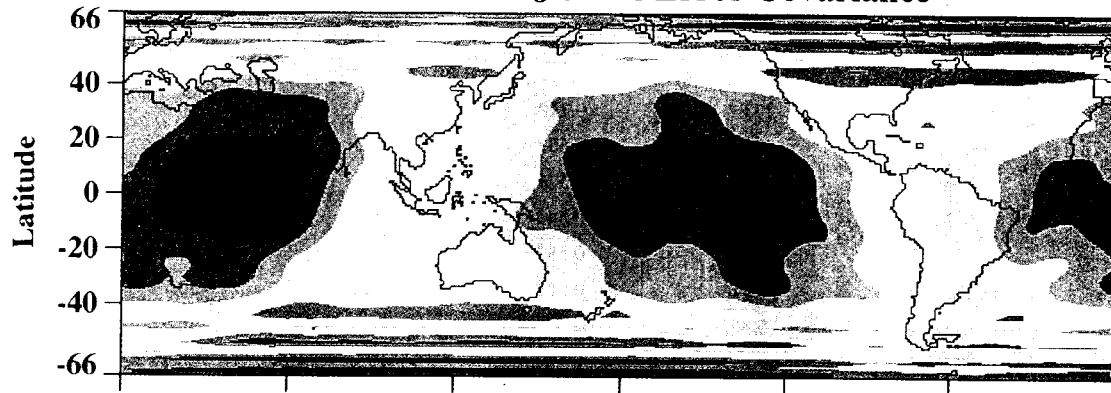
This evidence suggests that the JGM-2 error covariance is realistic and the radial orbit errors for T/P induced by gravity field mismodeling have been reduced to the 2-cm RMS level. This is a substantial accomplishment considering that the original 10-cm goal was once thought by some to be nearly unachievable. Certainly, one of the reasons the gravity-induced radial orbit errors for T/P are so small is the relatively high 1330 km altitude of the orbit. Given that future altimeter missions may be in lower orbits, an analysis of the performance of JGM-2 for a few of these candidate orbits is warranted.

#### Predicted Performance for ERS 1 and Seasat/Geosat

The performance of JGM-2 for the orbits of ERS 1, Geosat, and Seasat is important not only for the analysis of altimeter data from those missions but also for the planning of future missions which may be considering these orbits. Tables 8 and 9 show the predicted orbit errors in the radial, cross-track, and along-track directions using the JGM-2 error covariance for ERS 1 and Geosat/Seasat, respectively. Since the JGM-2 error covariance has been shown to be realistic for T/P, these results indicate that JGM-2 would introduce radial orbit errors of less than 10 cm RMS for either orbit. JGM-2 does not include SLR tracking data from ERS-1, so the performance for ERS-1 could be improved in the future when these data are added, although the SPOT 2 DORIS tracking data has probably well defined the model at this inclination/altitude with the exception of the zonal and resonant coefficients, which can be improved. In any case, errors due to the mismodeling of nonconservative forces will likely be larger than those caused by gravity mismodeling using the JGM-2 model. Figure 5 shows the radial orbit error performance of JGM-2 versus inclination for satellites near the altitude of ERS 1 and Geosat/Seasat (800 km). These results

## TOPEX/Poseidon Mean Radial Orbit Errors

### Based on the JGM-1 Error Covariance



### Based on the JGM-2 Error Covariance

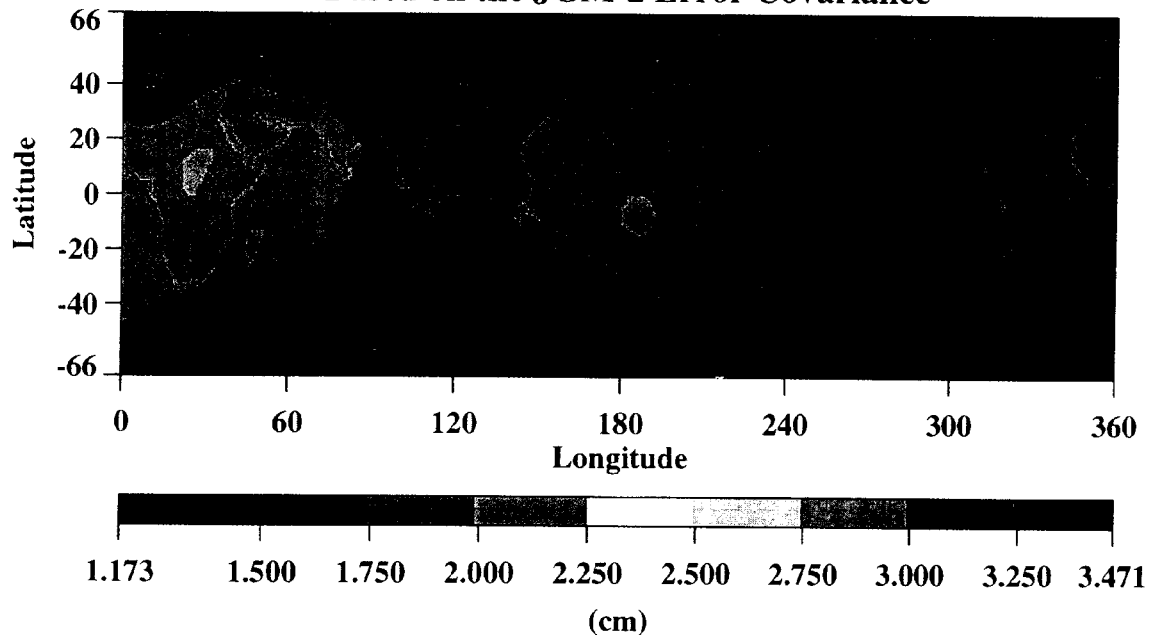


**Plate 1.** Mean radial orbit errors as a function of geographic location using the error covariance matrices for JGM-1 and JGM-2.

demonstrate that some improvement in JGM-2 is needed before it can provide the same radial accuracy for lower orbits that it provides for T/P. Of course, at lower altitude, atmospheric drag becomes an increasingly greater concern. While these improvements are possible, an approach less dependent on improving physical atmospheric models might be possible via the reduced-dynamic technique advocated by *Yunck et al.* [1994] using GPS data, although the performance required at these lower altitudes has not yet been demonstrated other than through covariance studies.

#### Predicted Performance for Other Geodetic Satellites

The performance of the JGM-2 model for nonaltimetric geodetic satellites is also of interest. Table 10 shows the predicted orbit performance of the JGM-2 model in the radial, transverse, and normal components for a variety of current geodetic satellites. The most precise of these are the SLR satellites LAGEOS, LAGEOS 2, Ajisai, Starlette, and the satellite recently launched by France into a SPOT-like orbit, Stella. Table 11 shows the results of fitting the SLR tracking data for these satellites for several test arcs using different gravity mod-

**Table 6. Orbital Performance for Different Gravitational Models for TOPEX/POSEIDON Cycle 32 (July 27 to August 6, 1993)**

Gravity Model	SLR Fit, cm	DORIS Fit, mm/sec	Crossover RMS, cm	Altimeter RMS, <sup>†</sup> cm
GEM-L2	105.89	2.607	105.6	
GEM-T1	31.42	0.979	38.5	
GEM-T2	17.84	0.710	21.8	
GEM-T3S	13.94	0.652	18.5	
JGM-1S	7.66	0.576	12.5	
JGM-2S	3.98	0.549	10.3	
GEM-T3	8.57	0.587	12.8	30.9
GEM-T3A	6.91	0.573	11.4	30.7
JGM-1	5.36	0.561	10.9	28.9
JGM-2	3.81	0.549	10.2	28.7
TEG-2B	16.68	0.666	16.3	34.1
OSU-91A	12.01	0.615	16.5	31.7
GRIM4-C3	14.05	0.689	18.2	39.4
WGS-84	17.74	0.700	18.4	55.0

Cycle 32 contained 8211 SLR observations, 56,072 DORIS observations, 5100 crossover observations, and 48,900 sampled altimeter points. The estimated parameters were position and velocity at epoch, a daily constant along-track acceleration, daily once-per-revolution accelerations in the along-track and normal directions, and a DORIS network timing bias.

<sup>†</sup> Fields extended to degree 70 using OSU91A when necessary. Altimeter data were corrected for high-degree geoid effects (degrees 71-360) using OSU91A. The altimeter fits represent the difference between the measured sea surface height and a model composed of the geoid plus a 20 x 20 of the *Levitus* [1982] dynamic topography model; these fits primarily reflect the level of geoid error in each of the models, but errors in the *Levitus* model also contribute. For the JGM models, these altimeter fits can be reduced to less than 20 cm using a T/P derived dynamic topography model.

**Table 7. RMS Differences of T/P Cycle 32 Orbits Derived From SLR and DORIS Data and a Given Gravity Model Versus the GPS Reduced-Dynamic Orbits Computed by JPL**

Gravity Model	Radial	Cross-Track	Along-Track
GEM-L2	69.1	84.6	250.5
GEM-T1	26.7	55.0	76.2
GEM-T2	14.9	24.3	41.2
GEM-T3S	11.9	14.4	31.4
JGM-1S	6.5	7.0	18.7
JGM-2S	2.9	7.2	9.7
GEM-T3	7.3	9.8	21.2
GEM-T3A	6.2	8.2	18.0
JGM-1	4.5	7.4	14.9
JGM-2	3.0	7.5	9.8
TEG-2B	12.5	12.6	36.2
OSU-91A	9.5	20.4	26.2
GRIM4-C3	13.0	15.6	40.0
WGS-84	12.8	24.1	41.0

Units in centimeters.

**Table 8. Predicted Orbit Error Due to JGM-2 Commission Errors for ERS 1/SPOT 2 ( $1\sigma$ )**

Gravity Model	Radial	Cross-Track	Along-Track
GEM-T1	268.4	218.8	3588.8
GEM-T2	119.7	130.6	1938.9
GEM-T3S	144.7	155.9	2316.2
GEM-T3SA	18.0	25.0	182.1
JGM-1S	16.1	22.8	184.5
JGM-2S	15.1	21.7	179.1
GEM-T3	83.2	85.0	1389.0
GEM-T3A	11.9	19.8	166.5
JGM-1	8.4	15.9	164.8
JGM-2	8.0	15.1	160.4

Zonal errors not included. Units in centimeters.

els. The tests for LAGEOS 2 and Stella are particularly enlightening since tracking data from these spacecraft are not present in any of the models tested. For Stella, along-track 1-CPR accelerations were estimated in the tests in order to remove the error due to the odd zonal coefficients and any residual error in the nonconservative force models. This was necessary since the SPOT 2 data used in the JGM models included the estimation of 1-CPR accelerations, thereby absorbing significant nonconservative force model error and most of the radial signal arising from the odd zonals. While errors in modeling the nonconservative forces acting on Stella are smaller (due to its spherical shape), if the 1-CPR accelerations are eliminated from the Stella tests, then the performance of the JGM models degrades significantly, and they are outperformed by models which processed SPOT 2 without the 1-CPR accelerations, such as TEG-2B. As an example, if the tests given in Table 11 are recomputed without estimating the 1-CPR empirical along-track accelerations, the fit using JGM-2 degrades to 54 cm, but the fit using TEG-2B degrades to only 41 cm. Tests conducted during the development of the JGM models indicated that not solving for the once-per-revolution accelerations on SPOT 2 degraded the performance of the gravity model for satellites at other inclinations, including T/P.

The Stella tests indicate the complex issues associated with the separation of conservative and nonconservative forces, the estimation of empirical parameters to accommodate these forces, and decisions which must be made during the development of the models in the context of satellite modeling and its effects on the gravity model performance.

These results demonstrate that gravity error is not a major error source for these satellites, with the exception of Stella, where significant improvement could be gained through the inclusion of its data in the gravity model. The reduction of the remaining gravity error for these satellites will probably depend on improved modeling of temporal variations in gravity [Nerem *et al.*, 1993b; Watkins and Eanes, 1993] and improvements in other background models.

#### Accuracy of the JGM Geoid Models

So far, we have only considered the accuracy of the JGM models in orbital applications. However, as stated at the outset, the accuracy of the JGM-2 geoid is also of interest for the computation of ocean dynamic topography using satellite altimeter data. Plate 2 shows the commission errors (the errors arising from only the coefficients to degree 70 and not including the

**Table 9. Predicted Orbit Error Due to JGM-2 Commission Errors for Geosat / Seasat ( $1\sigma$ )**

Gravity Model	Radial	Cross-Track	Along-Track
GEM-T1	44.2	75.4	272.5
GEM-T2	19.8	43.5	97.9
GEM-T3S	29.6	65.5	146.9
GEM-T3SA	24.5	56.2	139.2
JGM-1S	14.0	41.4	75.0
JGM-2S	12.3	39.2	66.0
GEM-T3	11.9	38.3	106.0
GEM-T3A	10.4	33.5	100.2
JGM-1	7.2	27.4	65.6
JGM-2	6.5	26.4	58.0

Zonal errors not included. Units in centimeters.

**Table 10. Predicted Orbit Error Due to Gravity for JGM-2 ( $1\sigma$ )**

Satellite	Radial	Cross-Track	Along-Track
Ajisai	2.6	3.6	13.2
LAGEOS	0.3	0.4	1.5
LAGEOS 2	0.5	0.5	1.7
Starlette	5.2	7.2	16.1
GEOS 3	6.6	9.6	72.5
GEOS 1	2.3	3.0	45.1
GEOS 2	3.3	5.1	63.8
Peole	98.1	106.7	353.5
BEC	9.2	11.4	60.0
DIC	14.5	16.9	70.7
DID	10.1	11.2	88.9
Oscar	13.0	17.1	65.8
NOVA	9.6	21.7	397.0

Zonal errors not included. Units in centimeters.

**Table 11. Orbit Fits to Satellite Laser Ranging Tracking Data Using Different Gravity Models**

Gravity Model	LAGEOS*	LAGEOS 2 <sup>†</sup>	Starlette <sup>‡</sup>	Ajisai <sup>§</sup>	Stella <sup>+</sup>
GEM-L2	6.41	11.38	174.18	88.73	352.36
GEM-T1	2.99	4.96	17.05	15.18	355.97
GEM-T2	2.85	3.94	12.02	8.95	273.26
GEM-T3S	2.80	6.18	10.77	8.34	296.53
JGM-1S	2.71	3.67	9.14	7.44	20.11
JGM-2S	2.73	3.62	9.05	7.46	18.78
GEM-T3	2.83	5.22	10.76	8.42	89.72
GEM-T3A	2.78	4.81	10.09	8.28	31.70
JGM-1	2.71	3.66	8.86	7.53	22.06
JGM-2	2.71	3.66	8.82	7.53	19.56
OSU-91A	2.90	3.83	11.87	8.89	124.44
TEG-2B	2.82	5.37	10.19	7.78	31.01
GRIM4-C3	2.70	3.71	10.14	8.38	109.40
WGS-84	11.77	26.40	109.74	56.02	321.46

RMS residuals in centimeters.

\*Test consists of three monthly arcs (April, May, and June 1988) estimating 5-day values of polar motion, all station coordinates except the latitude of GSFC and the latitude/longitude of Hawaii, the spacecraft state for each arc, solar pressure for each arc, and along-track accelerations every 15 days.

<sup>†</sup>Test consists of two monthly arcs (November and December 1992) estimating 5-day values of polar motion, all station coordinates except the latitude of GSFC and the latitude/longitude of Hawaii, the spacecraft state for each arc, along-track acceleration every 15 days, and a once-per-revolution along-track acceleration (cosine and sine) every 15 days (60-s integration step size).

<sup>‡</sup>Test consists of eight 5-day arcs (April 4 to May 14, 1989) estimating 5-day values of polar motion, the spacecraft state for each arc, a daily drag parameter, and solar pressure for each arc.

<sup>§</sup>Test consists of eight 5-day arcs (August 3 to September 19, 1988) estimating 5-day values of polar motion, the spacecraft state for each arc, a daily drag parameter, and solar pressure for each arc.

<sup>+</sup>Test consists of five 4-day arcs (September 30 to October 19, 1993) estimating 5-day values of polar motion (using all arcs together), the spacecraft state for each arc, a drag parameter and solar pressure for each arc, and a once-per-revolution along-track acceleration for each arc. The total 20-day data set consisted of 1260 SLR observations from 14 stations.

Geoid Height Errors for JGM-2

Contour Interval = 3.0 cm

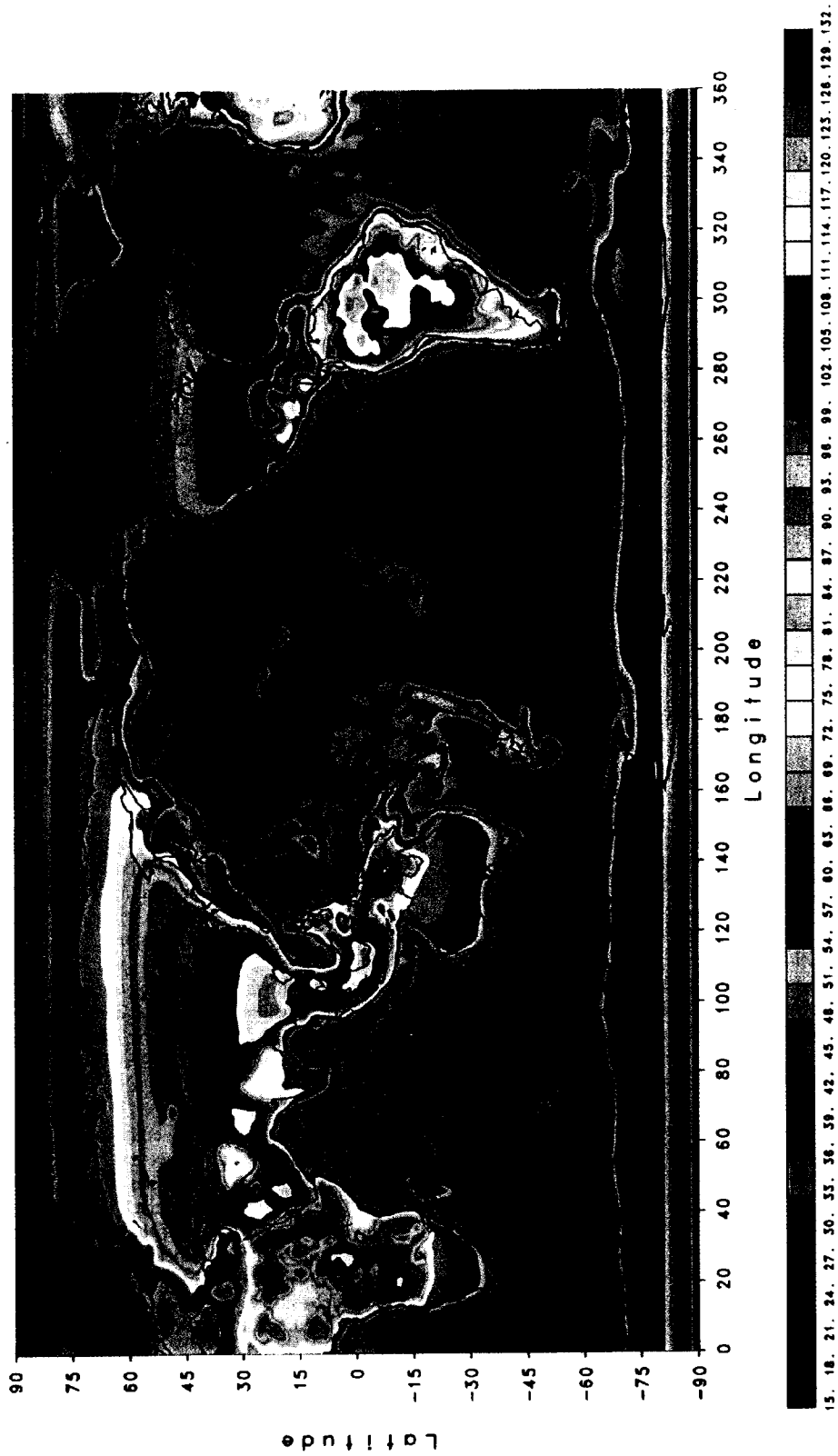
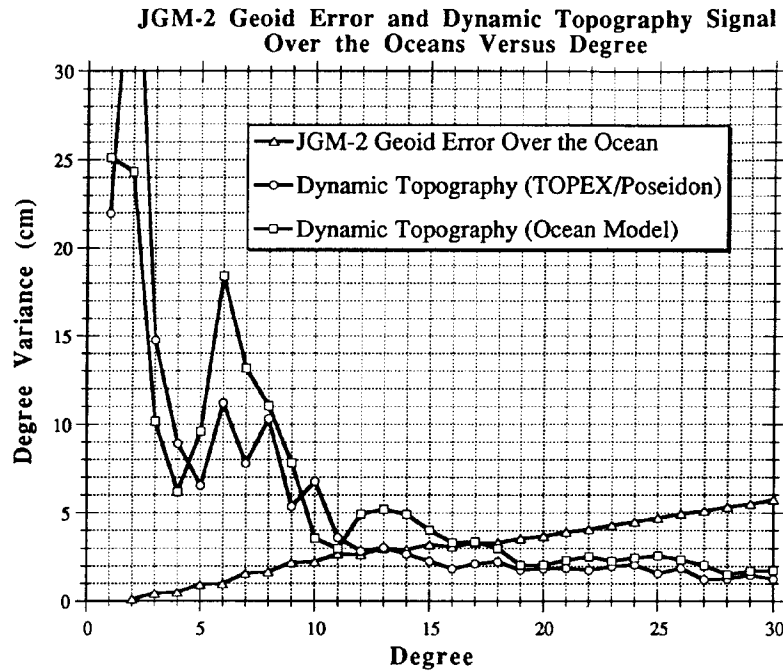


Plate 2. Predicted geoid commission errors using the JGM-2 error covariance matrix.



**Figure 6.** Comparison of JGM-2 geoid errors and dynamic topography signal by spherical harmonic degree over the oceans. Two models of ocean dynamic topography are shown; one determined from the first 19 cycles of TOPEX/POSEIDON data using the JGM-2 geoid; and another determined from a spherical harmonic expansion of a representative sample from the ocean model of *Semtner and Chervin* [1992], which was forced with *Levitus* [1982] climatology.

omission error, which arises from higher degree terms due to truncation of the model at degree 70) of the geoid complete to degree 70 computed using the JGM-2 error covariance (the geoid error for JGM-1 is nearly identical and thus will not be displayed). While the geoid commission error over the continents can exceed  $\pm 1$  m, the errors over the ocean area are generally at the  $\pm 25$  cm level. This predicted error is consistent with the T/P altimeter residuals shown in Table 6. Figure 6 shows a comparison of the JGM-2 ocean geoid error and the signal of the dynamic topography versus spherical harmonic degree. The geoid error exceeds the signal of the dynamic topography at about degree 15. While geoid error does not affect the determination of the temporal variations of the dynamic topography, it is clearly the main limitation in computations of the mean dynamic topography, especially in light of the reduction in orbit error for the T/P mission versus previous missions. The work by *Nerem et al.* [this issue] contains a more thorough discussion on the use of JGM-2 for determining the dynamic topography using T/P data. However, it is clear that with the improved accuracy of the T/P sea level measurements relative to previous missions, errors in the geoid are the largest remaining obstacle to determining the ocean dynamic topography using satellite altimetry.

#### Mean Gravity Anomalies From JGM-2

While the JGM models have been developed for T/P precision orbit determination, they also have a general use as one of the most accurate long-wavelength gravitational models available. The gravity anomalies from the JGM-2 model are of particular interest for geophysicists and other Earth scientists.

Plate 3 shows a map of the gravity anomalies computed from JGM-2. The altimeter and surface gravity data used in this model were corrected for truncation effects from degrees 71 to 360 using the OSU91A model of *Rapp et al.* [1991]. In computing the mean free-air gravity anomalies (Plate 3), it was necessary to apply a Pelin smoothing factor,  $\beta_{\eta}$  ( $\psi = 2.8^{\circ}$ ) [cf. *Katsambalos*, 1979; *Sjoberg*, 1980]. This smoothing removes the effects of leakage at higher frequencies. This effect is due to the above correction factor and accounts for the fact that truncating in spherical harmonics is not simply equivalent to changing the block size when computing mean gravity anomalies. A more detailed gravity anomaly map with resolution down to  $0.5^{\circ}$  could be computed by augmenting the JGM-2 harmonics with those of OSU91A through degree 360. The predicted gravity anomaly commission errors using the JGM-2 error covariance have a geographic distribution similar to the geoid errors (Plate 2), with the errors ranging from a few milligals over the oceans to as much as 8 mGal over the continents. The uneven distribution of the errors reflects the distribution and accuracy of the altimeter and surface gravity data used in the JGM-2 solution. In the future, the release of previously classified surface gravity data should improve the gravity model accuracy in many of the poorly observed regions shown in Plate 2.

#### Conclusions and Future Work

The development of the JGM-2 gravity model represents a major advance in modeling of the Earth's gravitational field, especially with regard to its performance for T/P orbit determi-

# Mean Free Air Gravity Anomalies for JGM-2

Contour Interval = 4.0 mgals



Plate 3. Mean gravity anomalies for the JGM-2 model using a Pelineen smoothing factor,  $\beta_n$  ( $\psi = 2.8^\circ$ ) [cf. Katsambalos, 1979; Sjoberg, 1980].

nation. It will be extremely difficult to reduce the 2-cm RMS radial orbit error performance currently achieved for T/P, although the inclusion T/P GPS tracking data in the model will probably produce some improvement [Schutz *et al.*, 1994; Christensen *et al.*, 1994]. However, despite the success with T/P orbit determination, there is considerable room for improvement in the model including the following:

1. The improvement of the marine geoid for computations of ocean dynamic topography using altimeter data is crucial for oceanographic research. Currently, geoid error exceeds the signal of the dynamic topography for wavelengths shorter than about 2500 km. Improvement of the marine geoid should be one of the highest priorities for gravity model research in the future, but will probably have to wait for a dedicated gravitational field mission before significant improvements are realized.

2. Improvement of the gravity field for orbit determination of low (~800 km) altimeter satellites such as ERS 1, ERS 2, and Geosat Follow-On is needed if T/P-type performance is expected to be achieved. Gravity-induced radial orbit errors at the decimeter level still limit the orbit determination accuracies which may be achieved for these missions. Altimeter missions at this altitude are desirable because of their lower cost; however, achieving T/P orbit accuracies will require either large improvements in the gravitational and nonconservative force models, or less model-dependent techniques such as have been proposed by Yunck *et al.* [1994] using GPS tracking.

3. Improvement of the short-wavelengths of the gravity model over the continents is needed. Clearly, the gravity field is known much better over the oceans (due to satellite altimetry) than over the continents.

4. The zonal and satellite-specific resonant coefficients, which have the largest effect on the satellite orbits, produce perturbations which are difficult to separate from errors in the modeling of nonconservative forces acting on the satellites. The adjustment of empirical terms to accommodate these non-conservative orbit errors also absorbs the zonal and resonant gravity signal, thus degrading the gravity solution for these coefficients. Improvements in the modeling of nonconservative forces will help separate these terms.

Over the next several years, there are many improvements which are expected to be made to improve the above limitations of the JGM models including the following:

1. Substantial improvements in the continental areas may be realized in the next several years as surface gravity data from the former Soviet Union, China, and other areas which were previously unavailable or classified becomes available to the civilian scientific community.

2. The inclusion of ERS 1 and T/P altimetry alone may significantly improve the JGM models. ERS 1 altimetry provides high-latitude data not previously present in the JGM models. In addition, ERS 1's planned 168-day repeat orbit will provide unprecedented spatial resolution. The T/P altimetry will also be extremely valuable due to its state-of-art ionosphere and wet troposphere corrections, as well as other improvements over previous missions.

3. The improved accommodation of temporal variations in gravity may be crucial for any future advances in modeling the static field. Many of the coefficients describing the long-wavelengths of the gravity field are known to the same level as their measured temporal variations [Nerem *et al.*, 1993b], thus any improvement will depend on better accommodation of these variations than was accomplished in the JGM models. This can be accomplished through either geophysical modeling of

the variations [Chao and Au, 1991; Chao, 1993] or estimation of the variations simultaneously in the gravity solution using long time series of data. Progress in both of these areas [Nerem *et al.*, 1993b; Gegout and Cazenave, 1993; Watkins and Eanes, 1993; Chao and Eanes, 1994] promises to provide improvements in the JGM models in the coming years.

4. The inclusion of T/P GPS tracking data will provide an incremental improvement to the JGM models, but this improvement will likely be small and most noticeable for T/P orbits [Schutz *et al.*, 1994]. SLR tracking data from ERS 1 and Stella should also improve the performance of the JGM models for Sun synchronous orbits.

Late in this decade, the proposed Gravity and Magnetics Earth Surveyor mission [Frey *et al.*, 1993] could provide unprecedented improvements in the model of the Earth's gravitational field. Until then, improvements will be largely incremental, although much can be accomplished in this manner as evidenced by the T/P example. The combined efforts of many institutions which propelled the gravity model improvements for T/P might also serve as an example for future efforts striving to determine the time-variable distribution of the Earth's mass and its affect on satellite orbits, the oceans, and the Earth's climate.

**Acknowledgments.** The JGM gravity models were named for the late James G. Marsh, whose leadership of this research activity and collaborations with other research institutions made it all possible. The GSFC Group also wants to especially acknowledge one of our co-authors, Girish Patel, who has shown great strength and grace in the face of adversity. In spirit, his fight is our own. We thank the following individuals for their contributions to the computation of the JGM gravity models: T. L. Felsentregger, B. V. Sanchez, D. S. Chinn, N. L. Chandler, L. Gehrmann, S. Kapoor, J. J. McCarthy, K. E. Rachlin, and D. E. Pavlis. G. W. Rosborough assisted in the evaluations of the gravity models and E. J. Schrama helped with preparing some of the figures. G. H. Born and his group were instrumental in developing the finite element force model for T/P. We thank the French Space Agency, CNES, for providing the DORIS tracking data for TOPEX/POSEIDON and SPOT 2. The support of D. E. Smith in the pursuit of this activity is gratefully acknowledged. This research was funded by the TOPEX Project at the Jet Propulsion Laboratory and the Solid Earth Sciences Branch at NASA Headquarters. Questions regarding the development and use of any of the models discussed in this paper may be directed to the first author via the internet at snerem@santafe.gsfc.nasa.gov.

## References

- Antreasian, P. G., and G. W. Rosborough, Prediction of radiant energy forces on the TOPEX/POSEIDON spacecraft, *J. Spacecr. and Rockets*, 29(1), 81-90, 1992.
- Barlier, F., C. Berger, J. Falin, G. Kockarts, and G. Thuillier, A thermospheric model based on satellite drag data, *Aeron. Acta*, 185, 1977.
- Bertiger, W. I., et al., GPS precise tracking of TOPEX/POSEIDON: Results and implications, *J. Geophys. Res.*, this issue.
- Boucher, C., Z. Altamimi, and L. Duhem, ITRF92 and its associated velocity field, *IERS Tech. Note* 15, Obs. de Paris, October 1993.
- Brosche, P., J. Wunsch, J. Campbell, and H. Schuh, Ocean tide effects in universal time detected by VLBI, *Astron. Astrophys.*, 245, 676-682, 1991.
- Casotto, S., Ocean tide models for TOPEX precise orbit determination, Ph.D. dissertation, Univ. of Tex. at Austin, 1989.

- Cazenave, A., J. J. Valette, and C. Boucher, Positioning with DORIS on SPOT-2 after the first year of mission, *J. Geophys. Res.*, **97**, 7109-7119, 1992.
- Chao, B. F., The geoid and Earth rotation, in *Geoid and Its Geophysical Interpretations*, edited by P. Vanicek and N. T. Christou, pp. 285-298, CRC Press, Boca Raton, Fla., 1993.
- Chao, B. F., and A. Y. Au, Temporal variation of Earth's zonal gravitational field caused by atmospheric mass redistribution: 1980-1988, *J. Geophys. Res.*, **96**, 6569-6575, 1991.
- Chao, B. F., and R. Eanes, Global gravitational changes due to atmospheric mass redistribution as observed by Lageos' nodal residual, *Geophys. J. Int.*, in press, 1994.
- Cheng, M. K., R. J. Eanes, C. K. Shum, B. E. Schutz, and B. D. Tapley, Temporal variations in low degree zonal harmonics from Starlette orbit analysis, *Geophys. Res. Lett.*, **16**(5), 393-396, 1989.
- Cheng, M. K., R. J. Eanes, and B. D. Tapley, Tidal deceleration of the moon's mean motion, *Geophys. J. Int.*, **109**, 401-409, 1992.
- Christensen, E. J., B. J. Haines, K. C. McColl, and R. S. Nerem, Observations of geographically correlated orbit errors for TOPEX/POSEIDON using the global positioning system, *Geophys. Res. Lett.*, in press, 1994.
- Christodoulidis, D. C., D. E. Smith, R. G. Williamson, and S. M. Klosko, Observed tidal braking in the Earth/Moon/Sun system, *J. Geophys. Res.*, **93**, 6216-6236, 1988.
- Degnan, J. J., Millimeter accuracy satellite laser ranging: A review, in *Contributions of Space Geodesy to Geodynamics: Technology*, vol. 25, pp. 133-162, AGU, Washington, D.C., 1993.
- DeMets, C., R. G. Gordon, D. F. Argus, and S. Stein, Current plate motions, *Geophys. J. Int.*, **101**, 425-478, 1990.
- Denker, H., and R. H. Rapp, Geodetic and oceanographic results from the analysis of 1 year of Geosat data, *J. Geophys. Res.*, **95**, 13151-13168, 1990.
- Eanes, R. J., and M. M. Watkins, The CSR93L01 Solution, in *IERS Annual Report for 1992*, Obs. de Paris, 1993.
- Englar, T. S., R. H. Estes, D. C. Chinn, and G. A. Maslyar, ERODYN program mathematical description version 7809, Bus. Technol. Syst. Contract. Rep., BTS-TR-78-69, GSFC, Greenbelt, MD, September 1978.
- Frey, H., et al., GAMES: A gravity and magnetics experiment satellite for oceanography and solid earth science, *Eos Trans. AGU*, **74**, (16), 97, 1993.
- Gegout, P., and A. Cazenave, Temporal variations of the earth gravity field for 1985-1989 derived from LAGEOS, *Geophys. J. Int.*, **114**, 347-359, 1993.
- Gross, R. S., The effect of ocean tides on the Earth's rotation as predicted by the results of an ocean tide model, *Geophys. Res. Lett.*, **20**(4), 293-296, 1993.
- Heck, B., An evaluation of some systematic error sources affecting terrestrial gravity anomalies, *Bull. Geod.*, **64**, 88-108, 1990.
- Heiskanen, W., and H. Moritz, *Physical Geodesy*, W. H. Freeman, New York, 1967.
- Herring, T. A., and D. Dong, Measurement of diurnal and semidiurnal rotational variations and tidal parameters of the Earth, *J. Geophys. Res.*, in press, 1994.
- Huang, C., J. C. Ries, B. D. Tapley, and M. M. Watkins, Relativistic effects for near-Earth satellite orbit determination, *Cell. Mech. Dyn. Astron.*, **48**, 167-185, 1990.
- Katsambalos, K. E., The effect of the smoothing operator on potential coefficient determinations, Rep. 287, Dep. of Geod. Sci. and Surv., Ohio State Univ., Columbus, 1979.
- Kaula, W., *Theory of Satellite Geodesy*, Blaisdell, Waltham, Mass., 1966.
- Knocke, P. C., J. C. Ries, B. D. Tapley, Earth radiation pressure effects on satellites, *AIAA J.*, 1-11, 1988.
- Lambeck, K., Polar motion from the tracking of close earth satellites, in *Rotation of the Earth*, edited by P. Melchior and S. Yumi, pp. 123-127, 1972.
- Lerch, F. J., Optimum data weighting and error calibration for estimation of gravitational parameters, *Bull. Geod.*, **65**, 44-52, 1991.
- Lerch, F. J., S. M. Klosko, R. E. Laubscher, and C. A. Wagner, Gravity model improvement using GEOS 3 (GEM 9 and 10), *J. Geophys. Res.*, **84**, 3897-3915, 1979.
- Lerch, F. J., S. M. Klosko, and G. B. Patel, Gravity model development from LAGEOS, *Geophys. Res. Lett.*, **9**(11), 1263-1266, 1982.
- Lerch, F. J., S. M. Klosko, C. A. Wagner, and G. B. Patel, On the accuracy of recent Goddard gravity models, *J. Geophys. Res.*, **90**, 9312-9334, 1985.
- Lerch, F. J., J. G. Marsh, S. M. Klosko, E. C. Pavlis, G. B. Patel, D. S. Chinn, and C. A. Wagner, An improved error assessment for the GEM-T1 gravitational model, *J. Geophys. Res.*, **96** 20023-20040, 1991.
- Lerch, F. J., R. S. Nerem, D. S. Chinn, J. C. Chan, G. B. Patel, and S. M. Klosko, New error calibration tests for gravity models using subset solutions with independent data: Applied to GEM-T3, *Geophys. Res. Lett.*, **20**(2), 249-252, 1993a.
- Lerch, F. J., R. S. Nerem, B. H. Putney, S. M. Klosko, G. B. Patel, R. G. Williamson, H. B. Iz, J. C. Chan, and E. C. Pavlis, Improvements in the accuracy of Goddard Earth models (GEM), in *AGU Crustal Dynamics Monograph, Contributions of Space Geodesy to Geodynamics: Earth Dynamics*, **24**, 191-212, AGU, Washington, D.C., 1993b.
- Lerch, F. J., et al., Geopotential models from satellite tracking, altimeter, and surface gravity data: GEM-T3 and GEM-T3S, *J. Geophys. Res.*, **99**, 2815-2839, 1994.
- Levitus, S., Climatological Atlas of the World Ocean, *NOAA Prof. Pap. 13*, 173 pp., 1982.
- Luthcke, S. B., and J. A. Marshall, Nonconservative force model parameter estimation strategy for TOPEX/POSEIDON precision orbit determination, *NASA Technical Memo. 104575*, November 1992.
- Marsh, J. G., et al., A new gravitational model for the Earth from satellite tracking data: GEM-T1, *J. Geophys. Res.*, **93**, 6169-6215, 1988.
- Marsh, J. G., et al., The GEM-T2 gravitational model, *J. Geophys. Res.*, **95**, 22043-22070, 1990a.
- Marsh, J. G., F. J. Lerch, C. J. Koblinsky, S. M. Klosko, J. W. Robbins, R. G. Williamson, and G. B. Patel, Dynamic sea surface topography, gravity and improved orbit accuracies from the direct evaluation of Seasat altimeter data, *J. Geophys. Res.*, **95**, 13129-13150, 1990b.
- Marshall, J. A., and S. B. Luthcke, Modeling radiation forces acting on TOPEX/POSEIDON for precision orbit determination, *J. Spacecr. Rockets*, **31**(1), 99-105, 1994.
- McCarthy, D. D. (Ed.), IERS standards 1992, *IERS Tech. Note 13*, Obs. de Paris, November 1992.
- McClure, P., Diurnal polar motion, *NASA Doc. X-592-73-259*, 1973.
- Melbourne, W. G., B. D. Tapley, and T. P. Yunck, The GPS flight experiment on TOPEX/POSEIDON, *Geophys. Res. Lett.*, in press, 1994.
- Nerem, R. S., B. D. Tapley, and C. K. Shum, Determination of the ocean circulation using Geosat altimetry, *J. Geophys. Res.*, **95**, 3163-3179, 1990.
- Nerem, R. S., B. H. Putney, J. A. Marshall, F. J. Lerch, E. C. Pavlis, S. M. Klosko, S. B. Luthcke, G. B. Patel, R. G. Williamson, and N. P. Zelensky, Expected orbit determination performance for the TOPEX/POSEIDON mission, *IEEE Trans. Geosci. Remote Sens.*, **31**(2) 333-354, 1993a.
- Nerem, R. S., B. F. Chao, A. Y. Au, J. C. Chan, S. M. Klosko, N. K. Pavlis, and R. G. Williamson, Time variations of the Earth's gravitational field from satellite laser ranging to LAGEOS, *Geophys. Res. Lett.*, **20**(7), 595-598, 1993b.
- Nerem, R. S., F. J. Lerch, R. G. Williamson, S. M. Klosko, J. W. Robbins, and G. B. Patel, Gravity model improvement using

- the DORIS tracking system on the SPOT 2 satellite, *J. Geophys. Res.*, **99**, 2791-2813, 1994a.
- Nerem, R. S., F. J. Lerch, S. M. Klosko, G. B. Patel, R. G. Williamson, and C. J. Koblinsky, Ocean dynamic topography from satellite altimetry based on the GEM-T3 gravity model, *Manuscr. Geod.*, in press, 1994b.
- Nerem, R. S., E. J. Schrama, C. J. Koblinsky, and B. D. Beckley, A preliminary evaluation of ocean topography from the TOPEX/POSEIDON mission, *J. Geophys. Res.*, this issue.
- Nouel, F., J. Bardina, C. Jayles, Y. Labruno, and B. Truong, DORIS: A precise satellite positioning doppler system, in *Astrodynamics 1987*, vol. 65, *Adv. Astron. Sci.*, edited by J. K. Solder et al., pp. 311-320, 1988.
- O'Donnel, T., and R. Whitt, Beginning of life (BOL) thermal-optical properties of TOPEX surfaces: Precision orbit determination (POD), *JPL Interoffice Memo. 35592RW.084*, Jet Propuls. Lab., Pasadena, Calif., July 21, 1992.
- O'Donnel, T., R. Whitt, and T. Jones, TOPEX/POSEIDON precision orbit determination (POD): Spacecraft thermal properties, JPL Task Implementation Plan, *Rep. X*, Jet Propuls. Lab., Pasadena, Calif., October 31, 1991.
- Pavlis, N. K., Modeling and estimation of a low degree geopotential model from terrestrial gravity data, *Rep. 386*, Dep. of Geod. Sci. and Surv., Ohio State Univ., Columbus, 1988.
- Pavlis, N. K., and R. H. Rapp, The development of an isostatic gravitational model to degree 360 and its use in global gravity modeling, *Geophys. J. Int.*, **100**, 369-378, 1990.
- Rapp, R. H., The need and prospect for a world vertical datum, *Proc. IAG Symp.*, **2**, 432-445, 1983.
- Rapp, R. H., and N. K. Pavlis, The development and analysis of geopotential coefficient models to spherical harmonic degree 360, *J. Geophys. Res.*, **95**, 21885-21911, 1990.
- Rapp, R. H., Y. M. Wang, and N. K. Pavlis, The Ohio State 1991 geopotential and sea surface topography harmonic coefficient models, *Rep. 410*, Dep. of Geod. Sci. and Surv., Ohio State Univ., Columbus, 1991.
- Reigber, C., Representation of orbit element variations and force function with respect to various reference systems, *Bull. Geod.*, **55**, 111-131, 1981.
- Ries, J. C., C. Huang, and M. M. Watkins, Effect of general relativity on a near-Earth satellite in the geocentric and barycentric reference frames, *Phys. Rev. Lett.*, **61**(8), 903-906, 1988.
- Ries, J. C., C. Huang, M. M. Watkins, and B. D. Tapley, Orbit determination in the relativistic geocentric reference frame, *J. Astron. Sci.*, **39**(2), 173-181, 1991.
- Ries, J. C., R. J. Eanes, C. K. Shum, and M. M. Watkins, Progress in the determination of the gravitational coefficient of the Earth, *Geophys. Res. Lett.*, **19**(6), 529-531, 1992.
- Ries, J. C., C. K. Shum, and B. D. Tapley, Surface force modeling for precision orbit determination, in *Environmental Effects on Spacecraft Positioning and Trajectories*, *Geophys. Monogr. Ser.*, **73**, 111-124, AGU, Washington, D.C., 1993.
- Rosborough, G. W., *Satellite orbit perturbations due to the geopotential*, *Rep. CSR-86-1*, Univ. of Tex. at Austin, January 1986.
- Rosborough, G. W., and T. M. Kelecy, Improved mean sea surface estimation by gravity field error covariance weighting, *Mar. Geod.*, **14**, 101-120, 1990.
- Rubincam, D. P., Postglacial rebound observed by LAGEOS and the effective viscosity of the lower mantle, *J. Geophys. Res.*, **89**, 1077-1087, 1984.
- Schanzle, A. F., J. E. Rovnak, D. T. Bolvin, and C. E. Doll, Orbit determination support of the ocean topography experiment (TOPEX)/POSEIDON operational orbit, paper presented at NASA/GSFC Flight Mechanics/Estimation Theory Symposium, GSFC, Greenbelt, MD, May 1992.
- Schutz, B. E., B. D. Tapley, P. A. M. Abusali, and H. J. Rim, Dynamic orbit determination using GPS measurements from TOPEX/POSEIDON, *Geophys. Res. Lett.*, in press, 1994.
- Schwintzer, P., et al., *A new Earth gravity field model in support of ERS-1 and SPOT-2: GRIM4-S1/C1*, final report to the German and French Space Agencies (DARA & CNES), Munich and Toulouse, 1991.
- Semtner, A. J., and R. M. Chervin, Ocean general circulation from a global eddy-resolving model, *J. Geophys. Res.*, **97**, 5493-5550, 1992.
- Shum, C. K., B. D. Tapley, D. N. Yuan, J. C. Ries, and B. E. Schutz, An improved model for the Earth's gravity field, in *Proceedings of the International Association of Geodesy Symposium 103, Gravity, Gradiometry and Gravimetry*, 97-108, Springer-Verlag, New York, 1990.
- Sjoberg, L., A recurrence relation for the  $\beta_n$  function, *Bull. Geod.*, **54**, 69-72, 1980.
- Smith, D. E., R. Kolenkiewicz, P. J. Dunn, J. W. Robbins, M. H. Torrence, S. M. Klosko, R. G. Williamson, E. C. Pavlis, N. B. Douglas, and S.K. Fricke, Tectonic motion and deformation from satellite laser ranging to LAGEOS, *J. Geophys. Res.*, **95**, 22013-22041, 1990.
- Stewart, R. L., L.-L. Fu, and M. Lefebvre, Science opportunities for the TOPEX/POSEIDON mission, *JPL Pub. 86-18*, Jet Propuls. Lab., Pasadena, Calif., July 15, 1986.
- Tapley, B. D., R. S. Nerem, C. K. Shum, J. C. Ries, and D. N. Yuan, Determination of the general circulation of the oceans from a joint gravity field solution, *Geophys. Res. Lett.*, **15**(10), 1109-1112, 1988.
- Tapley, B. D., C. K. Shum, D. N. Yuan, J. C. Ries, R. J. Eanes, M. M. Watkins, and B. E. Schutz, The University of Texas Earth gravity field model, paper presented at IUGG XX General Assembly, IAG Symp. G3, Gravity Field Determination from Space and Airborne Measurements, Vienna, Austria, August 12-24, 1991.
- Tapley, B. D., et al., Precision orbit determination for TOPEX/POSEIDON, *J. Geophys. Res.*, this issue.
- TOPEX Science Working Group, satellite altimetric measurements of the ocean, *NASA, JPL Doc. 400-111*, Jet Propuls. Lab., Pasadena, Calif., March 1, 1981.
- Wahr, J. M., Body tides on an elliptical rotating, elastic and oceanless Earth, *Geophys. J. R. Astron. Soc.*, **64**, 677-703, 1981a.
- Wahr, J. M., The forced nutations of an elliptical, rotating, elastic, and oceanless Earth, *Geophys. J. R. Astron. Soc.*, **64**, 705-727, 1981b.
- Wakker, K.F., Report by the subcommittee on intercomparison and merging of geodetic data, *Rep. LR-638*, Delft Univ. of Technol., May 1990.
- Watkins, M. M., and R. J. Eanes, Long term changes in the Earth's shape, rotation, and geocenter, *Adv. Space Res.*, **13**(1), 11251-11255, 1993.
- Watkins, M. M., J. C. Ries, and G. W. Davis, Absolute positioning using DORIS tracking of the SPOT-2 satellite, *Geophys. Res. Lett.*, **19**(20), 2039-2042, 1992.
- Wunsch, C., and E. M. Gaposchkin, On using satellite altimetry to determine the general circulation of the oceans with applications to geoid improvements, *Rev. Geophys.*, **18**, 725-745, 1980.
- Yi, Y., and R. H. Rapp, The October 1990  $1^\circ \times 1^\circ$  mean anomaly file including an analysis of gravity information from China, internal report, Dep. of Geod. Sci. and Surv., Ohio State Univ., Columbus, February 1991.
- Yoder, C. F., J. G. Williams, J. O. Dickey, B. E. Schutz, R. J. Eanes, and B. D. Tapley, Secular variation of Earth's gravitational harmonic  $J_2$  from LAGEOS and nontidal acceleration of Earth rotation, *Nature*, **303**(5920), 757-762, 1983.

- Yuan, D., The determination and error assessment of the Earth's gravity field model, Ph.D. dissertation, Univ. of Tex. at Austin, May 1991.
- Yunck, T. P., W. I. Bertiger, S. C. Wu, Y. Bar-Sever, E. J. Christensen, B. J. Haines, S. M. Lichten, R. J. Muellerschoen, Y. Vigue, and P. Willis, First assessment of GPS-based reduced dynamic orbit determination on TOPEX/POSEIDON, *Geophys. Res. Lett.*, 21(7), 541-544, 1994.
- R. J. Eanes, J. C. Ries, B. E. Schutz, C. K. Shum, B. D. Tapley, and M. M. Watkins, Center for Space Research, University of Texas at Austin, Austin TX, 78712.
- F. J. Lerch, J. A. Marshall, R. S. Nerem, E. C. Pavlis, and B. H. Putney, NASA/GSFC Code 926, Space Geodesy Branch, Greenbelt, MD 20771. (e-mail: snerem@santafe.gsfc.nasa.gov).
- R. H. Rapp, Department of Geodetic Science and Surveying, Ohio State University, Columbus, OH, 43210.
- 
- R. Biancale and F. Nouel, Centre Nationale d'Etudes Spatiales, Toulouse, France.
- J. C. Chan, S. M. Klosko, S. B. Luthcke, G. B. Patel, N. K. Pavlis, and R. G. Williamson, Hughes STX Corporation, Greenbelt, MD, 20770.

(Received November 12, 1993; revised May 20, 1994; accepted May 20, 1994.)